OPTIMIZATION OF A TRANSLATING RIBOSOMAL AFFINITY PURIFICATION METHOD

A THESIS SUBMITTED TO
THE GRADUATE SCHOOL OF NATURAL AND APPLIED SCIENCES
OF
MIDDLE EAST TECHNICAL UNIVERSITY

BY

IRMAK GÜRCÜOĞLU

IN PARTIAL FULFILLMENT OF THE REQUIREMENTS
FOR
THE DEGREE OF MASTER OF SCIENCE
IN
BIOLOGY

FEBRUARY 2021

Approval of the thesis:

OPTIMIZATION OF A TRANSLATING RIBOSOMAL AFFINITY PURIFICATION METHOD

submitted by **IRMAK GÜRCÜOĞLU** in partial fulfillment of the requirements for the degree of **Master of Science** i**n Biology, Middle East Technical University** by,

Prof. Dr. Halil Kalıpçılar
Dean, Graduate School of **Natural and Applied Sciences** _____

Prof. Dr. Ayşe Gül Gözen
Head of the Department, **Biology** _____

Prof. Dr. A. Elif Erson Bensan
Supervisor, **Biology, METU** _____

Examining Committee Members:

Prof. Dr. Sreeparna Banerjee
Biology, METU _____

Prof. Dr. A. Elif Erson Bensan
Biology, METU _____

Assist. Prof. Dr. Bahar Değirmenci Uzun
Molecular Biology and Genetics, Bilkent University _____

Date: 10.02.2021

I hereby declare that all information in this document has been obtained and presented in accordance with academic rules and ethical conduct. I also declare that, as required by these rules and conduct, I have fully cited and referenced all material and results that are not original to this work.

Name, Last name : Irmak Gürcüoğlu

Signature :

ABSTRACT

OPTIMIZATION OF A TRANSLATING RIBOSOMAL AFFINITY PURIFICATION METHOD

Gürcüoğlu, Irmak
Master of Science, Biology
Supervisor : Prof. Dr. A. Elif Erson-Bensan

February 2021, 67 pages

Novel technologies revealed an immense transcriptome complexity in normal and in cancer cells. One of the reasons for this complexity is isoform variability in cancer cells. Transcript isoforms can arise due to alternative processing of the pre-mRNAs through alternative transcription start sites, alternative splicing, and alternative polyadenylation. To begin understanding how these isoforms may functionally contribute to the cancer phenotype, translation efficiency and coding potential of isoforms need to be established. Therefore, here, we optimized an assay where we captured translated mRNAs by immunoprecipitating active ribosome complexes that stably express a GFP tagged Ribosomal Protein L10A (RPL10A). We used magnetic bead conjugated Llama Anti-GFP VHH Single Domain Monoclonal Antibody to minimize unspecific interactions. Following immunoprecipitation, we isolated RNAs, cleaned DNA contamination, synthesized cDNA, and performed RT-qPCR. The optimized protocol was tested with non-coding RNAs and coding mRNAs. Hence, the optimization of this protocol allows individual and/or high throughput analysis of ribosome-associated mRNAs.

Keywords: RPL10A, TRAP, Ribosome, Polysome, Immunoprecipitation, eGFP

ÖZ

TRANSLASYONAL RIBOZOMLARIN AFİNİTE SAFLAŞTIRILMASININ OPTİMİZASYONU

Gürcüoğlu, Irmak
Yüksek Lisans, Biyoloji
Tez Yöneticisi: Prof. Dr. A. Elif Erson Bensan

Şubat 2021, 67 sayfa

Yeni teknolojiler, normal ve kanser hücrelerinde çok geniş transkriptom değişiklikleri ortaya çıkardı. Biz de kanser hücrelerinde izoform çeşitliliğinin sonuçlarını anlamakla ilgileniyoruz. Transcript çeşitliliği, Tek iplikli olgunlaşmamış mRNAların alternatif transkripsiyon başlangıç konumu, alternatif uçbirleştirme ve alternatif poliadenilasyonu sonucuunda oluşabilir. Bu izoformların kanser fenotipine nasıl katkı sağlayabileceğini anlamak için, izoformların kodlama potansiyellerini belirlemek gerekmektedir. Bu sebeple, biz burada, kalıcı olarak GFP etiketli Ribozom Protein L10A'yi ifade eden aktif ribozom komplekslerini immunoçöktürerek translasyona uğrayan mesajcı RNA'ları yakalıyoruz. Spesifik olmayan etkileşimleri en aza indirmek için magnetik boncuk konjuge monoklonal anti-GFP VHH tek domainli lama antikoru kullanıyoruz. İmmunoçöktüme sonrası, RNA izole ettik, DNA kirliliğini temizledik, cDNA sentezledik ve RT-qPCR yaptık. Optimize ettiğimiz protokol protein kodlamayan ve protein kodlayan RNAlar ile test edildi. Sonuç olarak, bu protokolün optimizasyonu, ribozomla etkileşen mRNAların bireysel ve/veya yüksek verimli analizine izin vermektedir.

Anahtar Kelimeler: RPL10A, TRAP, Ribozom, Polizom, İmmunoçöktürme, eGFP

To my family,

ACKNOWLEDGMENTS

First and foremost, I would like to express my deepest appreciation to my supervisor Prof. Dr. A. Elif Erson-Bensan, for her support, motivation, patience, and immense knowledge. Her perspective and advice helped me to become a better researcher.

I would like to thank my thesis committee members, Prof. Dr. Sreeparna Banerjee, and Assist. Prof. Dr. Bahar Değirmenci Uzun.

I thank Dr.Deniz Cansen Kahraman for the FACS analysis using BD FACSMelody in the Cancer Systems Biology Laboratory (CanSyL-METU).

I would like to thank members of the Muyan Lab, Banerjee Lab, Gürsel Lab and Terzi Lab for sharing their resources.

I am deeply thankful to Murat Erdem for his endless patience, immense knowledge, and help during my MSc study.

I am extremely grateful to Esra Çiçek, Mustafa Çiçek, Ayça Çırçır Hatıl, and Murat Erdem for their friendship, advice, and emotional support during my MSc study.

Many thanks to previous and current ERSON Lab members for their advice, friendship, and fun-filled working environment.

I am deeply thankful to my beloved Hamza Eray for his endless emotional support, advice, and jokes throughout my experiments and thesis writing process.

Last but not least, I am truly grateful to my mother Süreyya Gürcüoğlu, my father Selçuk Gürcüoğlu, my brother Uğur Gürcüoğlu for their endless support and belief throughout my life. Special thanks to our family cat Ponçik for its warm and funny existence.

TABLE OF CONTENTS

LIST OF TABLES

TABLES

LIST OF FIGURES

FIGURES

LIST OF ABBREVIATIONS

ABBREVIATIONS

TRAP: Translating Ribosomal Affinity Purification

IP: Immunoprecipitation

snoRNA: Small nucleolar RNA

TSS: Transcription Start Site

APA: Alternative Polyadenylation

AS: Alternative Splicing

ORF: Open Reading Frame

UTR: Untranslated Region

HEK293: Human Embryonic Kidney 293

eGFP: Enhanced Green Fluorescent Protein

FUNCAT: Fluorescent Noncanonical Amino Acid Tagging

SUnSET: Surface Sensing of Translations

TRICK: Translating mRNA Imaging by Coat Protein Knock Off

LIST OF SYMBOLS

SYMBOLS

RPL10A: Ribosomal Protein L10A

HNRNPA1: Heterogeneous Nuclear Ribonucleoprotein A1

XIST: X-inactive Specific Transcript

GAPDH: Glyceraldehyde 3-phosphate Dehydrogenase

RPLP0: 60S acidic ribosomal protein P0

MALAT1: Metastasis Associated Lung Adenocarcinoma Transcript 1

CHAPTER 1

INTRODUCTION

1.1 Ribosome Biogenesis

The eukaryotic ribosome (80S) consists of two main subunits, a large subunit which contains the 28S, 5.8S, 5S rRNA, and 46 ribosomal proteins and a small subunit that contains 18S RNA and 33 ribosomal proteins (Fromont-Racine, Senger, Saveanu, & Fasiolo, 2003). Ribosome biogenesis is initiated by the synthesis, processing, and assembly of ribosomal proteins and rRNAs. These distinct processes occur in the nucleolus first, then in the nucleus, and finally, in the cytoplasm.

5S ribosomal RNA is synthesized by RNA pol III, ribosomal proteins (r-proteins) are synthesized by RNA pol II. Ribosomal proteins are synthesized in the cytoplasm and then transported into the nucleus. RNA pol I transcribes 47S RNA which is later cleaved into 5.8S, 18S, and 28S rRNAs (Van Riggelen, Yetil, & Felsher, 2010).

From yeast to the human, eukaryotic ribosome biogenesis contains conserved rRNA and r-proteins and conserved non-ribosomal factors. These factors include small nucleolar RNPs (snoRNPs) and non-ribosomal proteins, which modify and process pre-rRNA, mediate RNP folding/remodeling, or facilitate protein association/ dissociation (Tschochner & Hurt, 2003). Pre-RNA processing can occur both co-transcriptionally and post-transcriptionally (Fernández-pevida, Kressler, & Cruz, 2014). In the post-transcriptional process, 35S pre-rRNA is synthesized first as a precursor for both ribosomal subunits and is present in 90S particles, including U3 sno-RNP containing processors (Figure1.1).

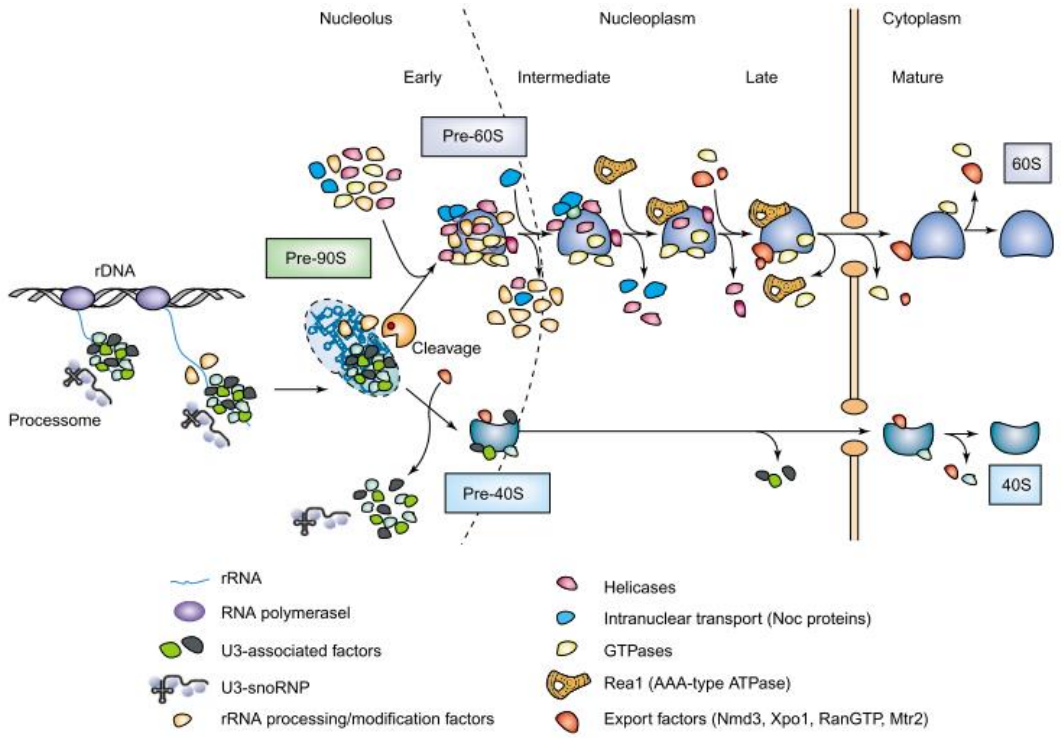

Figure 1.1 Post-transcriptionally processing of pre-rRNAs. The formation of pre-90S particle and transport of large and small subunits to the cytoplasm is shown. Pre-90S particles are formed in nucleolus to be disassembled to Pre-60S and Pre-40S later. In the nucleoplasm, the Pre-60S particles interact with ATPases, GTPases, helicases, and export factors. In the nucleoplasm, US-associated factor disassembly from Pre-40S follows export to the cytoplasm.Figure is taken from (Tschochner & Hurt, 2003).

In rapidly growing cells, processing of pre-rRNA occurs co-transcriptionally (Tollervey & Kos, 2010). rRNA undergoes covalent modifications by snoRNPs such as pseudouridylation and 2´-O- ribose methylation. In the small subunit assembly, SSU (small ribosomal subunit) processome is formed by chemical modification of pre-rRNA to 18S rRNA. U3 snoRNA has an important role in providing spatial constraints. In addition, many factors have transient roles in the biogenesis of the small subunit. Nucleases cleave the pre-rRNA at A_0, A_1, A_2 cleavage sites.

Large subunit assembly starts co-transcriptionally with covalent modifications of pre-rRNA with snoRNPs. Simultaneously, pre-rRNA is folded into a more compact

and stable conformation, and cleavage occurs. A great number of protein exchange occurs during the transition of small and large subunits from the nucleus to the cytoplasm. Pre-60S and pre-40s ribosomal subunits undergo final steps of maturation in the cytoplasm, remaining assembly factors are removed from the complex, and the last ribosomal proteins are added to ribosome subunits. Figure 1.2 shows 60S and 40S pre-ribosomal assembly and contribution of related factors.

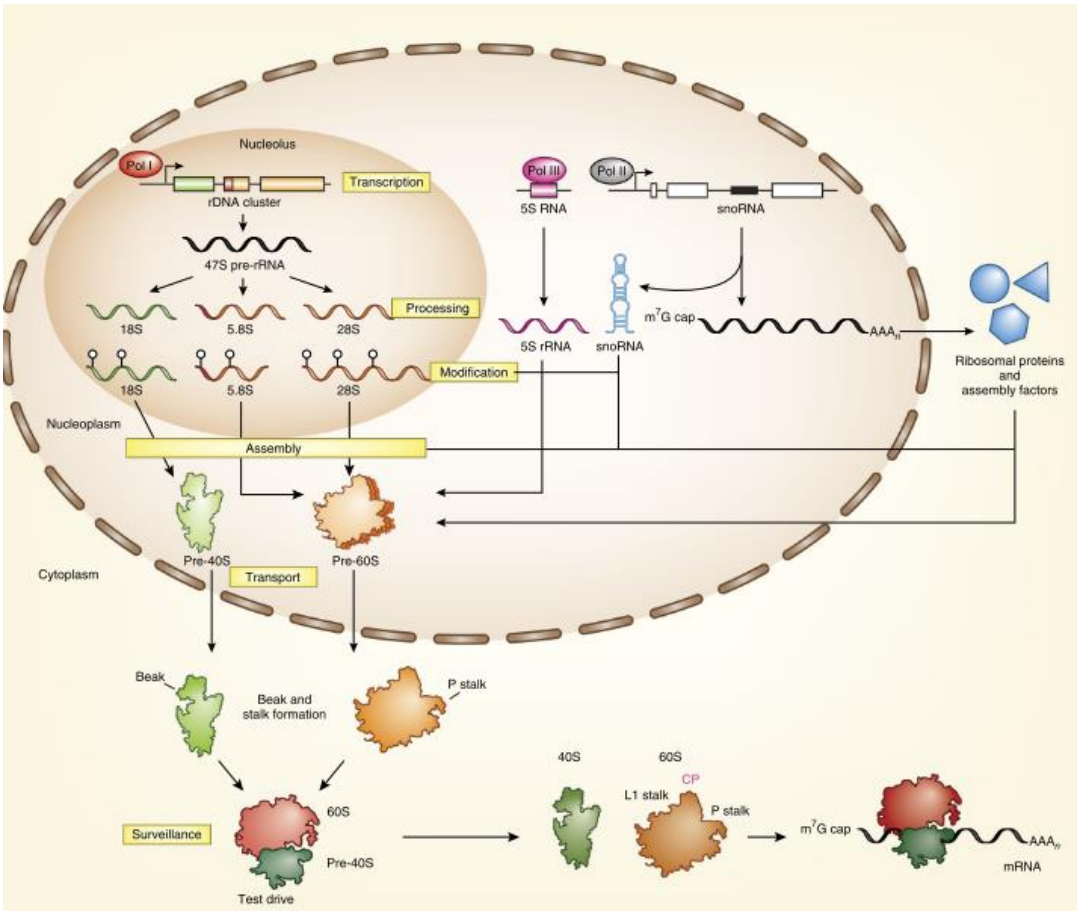

Figure 1.2 Assembly of the small and large ribosomal subunits. Ribosome biogenesis contains six important steps transcription of components, processing, assembly, and quality control and surveillance (Lafontaine, 2015).

1.1.1 RPL10A in Ribosomes

Similar to numerous factors involved in ribosome assembly, 60S ribosomal protein L10A (RPL10A) is also highly conserved among eukaryotes from protists to animals. RPL10A is found on the exit tunnel of 80S ribosomes. Given its structural role in translating ribosomes, RPL10A has been used as an adaptor for ribosome profiling and translating ribosomal affinity purification (TRAP) experiments. Enhanced GFP (eGFP) tagged RPL10A is used for immunoprecipitation of polysomes (polyribosomes) with eGFP specific antibodies or beads in the TRAP experiment mentioned in section 1.2.2.2.

RPL10A may also aid the preferential translation of specific mRNAs by binding to their Internal Ribosome Entry Sites (IRES). These specific mRNAs belong to several functional groups, including extracellular matrix (ECM) organization and glycosphingolipid metabolic processes RPL10A enhances expression of genes promoting growth Insulin Like Growth Factor2 (IGF2), Pleiotrophin (PTN), Early Growth Response 1 (EGR1), and cancer metastasis genes such as PKN3 (Protein Kinase N3) (Shi et al., 2017).

1.2 Ribosome Related Assays

Translation is a crucial process that converts genetic information to proteins via ribosomes. Capturing translating mRNAs has proved better to reflect mRNA fates in terms of translation kinetics. Hence, various new techniques have been developed to investigate ribosome association and, hence, coding potential of RNAs (Chekulaeva & Landthaler, 2016). These techniques allow quantitative and high throughput analysis.

1.2.1 Imaging-Based Methods

To measure translation dynamics, detecting and measuring the product of translation is the most straightforward way. However, detecting only newly synthesized proteins is challenging because of preexisting proteins. Besides, the sub-cellular location of protein synthesis is another wondering question. Imaging-based translation detecting methods overcome these challenges and answer questions about the impact of local protein synthesis in polarized cells. Figure 1.4 shows the schematic representation of these techniques.

1.2.1.1 Nascent Peptide Imaging (SINAPS and NTC) and Translating mRNA Imaging by Coat Protein Knock Off (TRICK)

These techniques rely on real-time imaging and quantification of single RNA translation dynamics in living cells. Translation visualization system is based on bright, photostable small molecule dyes, antibody enhancement, and multiepitope protein tags (Morisaki et al., 2016). A plasmid encoding the large nuclear protein KDM5B N-terminally tagged with a 10X FLAG-tag containing a 24X MS2 tag in the 3'UTR is constructed in one of the nascent peptide imaging studies. GFP tagged anti-FLAG-tag antibodies bind to 10X FLAG-tag as translation occurs, but halo-tagged MS2 coat proteins provide constant mRNA visualization by binding to the MS2 step-loop sites (Bertrand et al., 1998; Darzacq et al., 2009). GFP and Halo signal provide visualization of translation via fluorescent microscope.

Translation rate, mobility of polysomes, the strength of the signal (brightness) of a nascent polypeptide of large nuclear protein KDM5B (1554 aa) and smaller proteins beta-actin (374 aa) and the core histone H2B (125 aa) were compared with this technique (Morisaki et al., 2016) (Figure 1.2). H2B polysomes move significantly faster than KDM5B polysomes. The distance between 3'UTR of polysomal mRNA and nascent polypeptide chains were also measured. The distance was the shortest in

KDM5B, suggesting polysomes are more globular shaped rather than elongated. Brightness varied the most, and KDM5B translation sites were brighter than H2B and beta-actin.

In a similar approach, SunTag fluorescent tagging system is a visualization technique that relies on the co-transfection of two reporter systems. In this assay, cells are co-transfected with 24 SunTag peptides followed by a gene of interest with a second construct expressing a GFP-tagged single-chain intracellular antibody (scFv-GFP) that binds to the SunTag peptide with high affinity (Yan et al., 2016) (Figure 1.3). The repetitive sequence of SunTag recruits up to 24 copies of scFv-GFP (Tanenbaum, Gilbert, Qi, Weissman, & Vale, 2014).

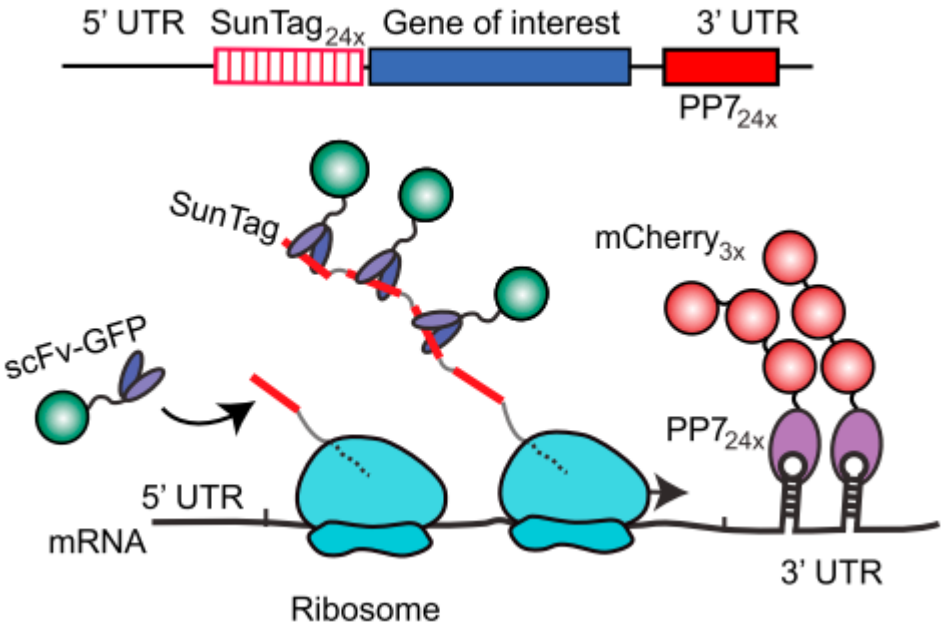

Figure 1.3 Schematic representation of nascent polypeptide labeling using the SunTag system and mRNA labeling using the PP7 (coat protein of bacteriophage PP7) system (Yan et al., 2016).

When the SunTag peptides emerge from the exit tunnel of ribosome during translation, fluorescent and soluble scFv-GFP immediately binds the SunTag. Simultaneously, the translated mRNA is fluorescently labeled with 24 copies of PP7

bacteriophage coat protein fused to three copies of mCherry (PP7-mCherry). PP7-mCherry fusion protein binds to a short hairpin sequence in the 3' UTR of the translated mRNA with high affinity (Chao, Patskovsky, Almo, & Singer, 2008) (Figure 1.3). This study showed heterogeneity in the translation properties of different mRNA isoforms of even the same gene in a single cell, as not translating, actively translating with many ribosomes, or bound to stalled ribosomes.

"Translating mRNA Imaging by Coat Protein Knock Off" (TRICK) method also distinguishes untranslated mRNA from previously translated ones in vitro. Similarly, bacteriophage PP7 and MS2 stem-loop is used to label specific transcripts within both coding sequence (PP7) and non-coding 3' Untranslated Region (3'UTR). PP7 coat protein is fused to nuclear localization signal (NLS-PCP-GFP) and MS2 coat protein is fused to NLS and red fluorescent protein RFP. In nucleus, single RNA appears yellow due to GFP and RFP signal, indicating that translation is not occurring. On the contrary, mRNAs appeared as red particles in the cytoplasm due to translation. TRICK allows detecting regulation and location of translated mRNA (Halstead, Wilbertz, Wippich, & Ephrussi, 2015). Figure 1.4 shows a schematic representation of the TRICK experiment.

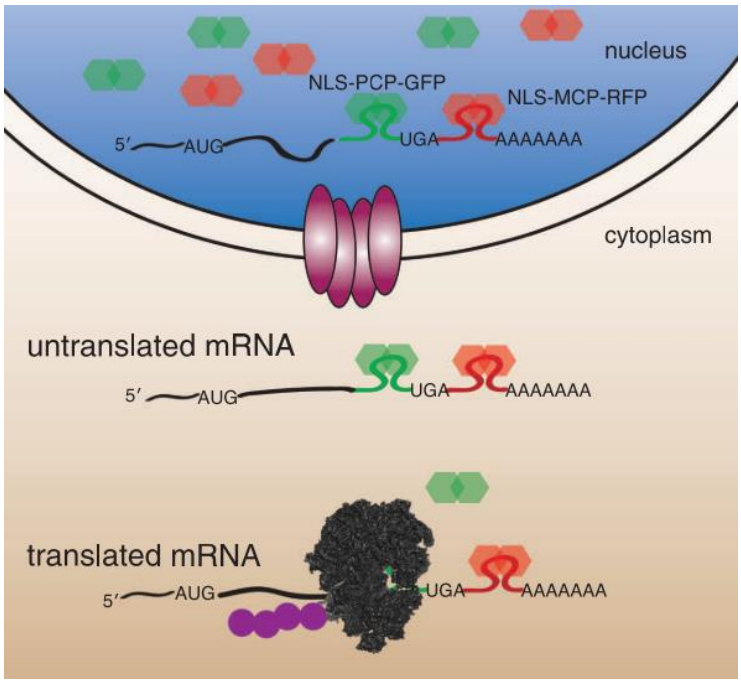

Figure 1.4 Schematic representation of TRICK assay. Untranslated mRNA appears yellow, and translated mRNA seems red (Halstead et al., 2015).

1.2.1.2 Fluorescent noncanonical amino acid tagging (FUNCAT), Surface Sensing of Translation (SUnSET) and FUNCAT-PLA and Puro PLA

Fluorescent non-canonical amino acid tagging (FUNCAT) can be applied to detect changes in protein synthesis and reveal the synthesized protein fate in different cellular localizations, *in situ*. Fluorescent tags Texas Red–PEO2–alkyne (TRA) and 5′-carboxyfluorescein–PEO8–azide (FLA) are designed by using polyethylene oxide (PEO) linker. TRA and FLA fluorescent alkyne probes are coupled with methionine surrogates, azidohomoalanine (AHA) and homopropargylglycine (HPG) (Dieterich et al., 2010). The FUNCAT process in hippocampal neurons includes methionine free medium incubation, the addition of AHA and HPG, fixation of cells with Triton X-100 and visualization.

SUnSET/ ribopuromycylation is a non-radioactive method to detect protein synthesis in cells. In this technique, translation inhibition is provided by puromycin treatment which is a structural analog of the aminoacyl tRNA incorporated into nascent polypeptide chain and prevents elongation (E. K. Schmidt, Clavarino, Ceppi, & Pierre, 2009). Puromycin treatment followed by immunostaining with anti-puromycin antibodies reveal translation location (David et al., 2012).

FUNCAT and puromycylation techniques are readvanced with the in situ proximity ligation assay based on the incidental co-localization of two antibodies connected to DNA oligonucleotides and guides the circularization of hybridized linker oligonucleotides (Dieterich et al., 2010). One of the antibodies is specific to the target protein, and the other is specific to the tag, such as puromycin and biotin (Dieck et al., 2015). FISH or rolling circle amplification provides detecting coincidence of two antibodies (Figure 1.5).

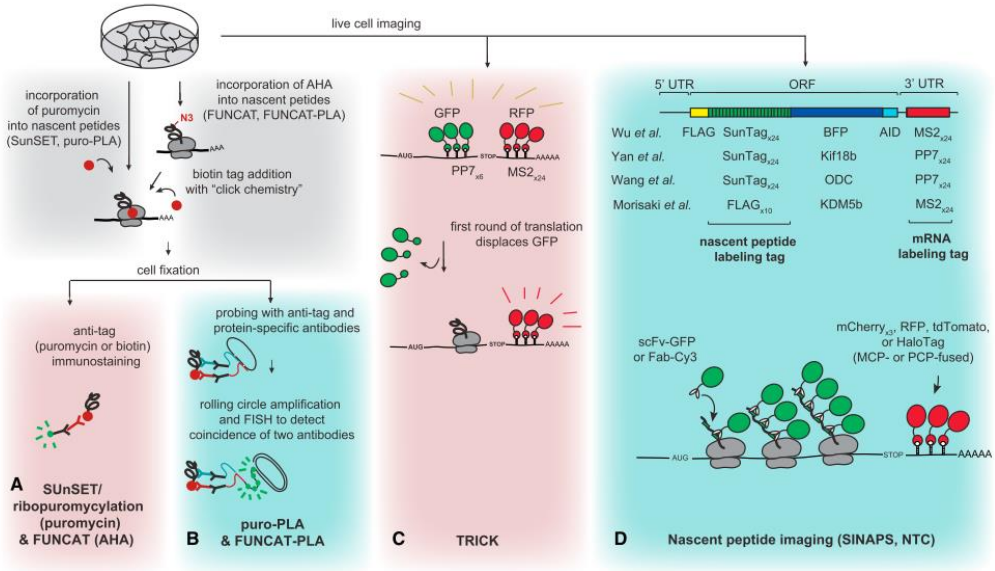

Figure 1.5 Imaging-based methods to quantify and visualize translation (Chekulaeva & Landthaler, 2016). A) SUnSET and FUNCAT assay, nascent peptides are labeled with the incorporation of puromycin. B) Puro-PLA and FUNCAT-PLA, the nascent polypeptide is tagged with tag and peptide-specific antibodies, and rolling circle amplification and FISH provide detecting. C) TRICK, GFP, and RFP signals indicate translation status of mRNAs. D) Nascent peptide imaging, scFv-GFP binds to nascent polypeptide chain as translation occurs.

1.2.2 RNA-seq Based Methods

mRNA and ribosome complex is a fragile structure and prone to dissociation due to non-covalent interactions. To overcome this problem and to analyze the translating mRNAs, techniques were developed such as polysome profiling, full-length translating mRNA profiling (RNC-seq), translating ribosome affinity purification (TRAP), proximity-based ribosome profiling, and ribosome profiling (Ribo-seq) (J. Zhao, Qin, Nikolay, Spahn, & Zhang, 2019). In this section, RNA-seq based methods are reviewed. In Figure 1.6. schematic representation of RNA-seq based translatom detection methods is given.

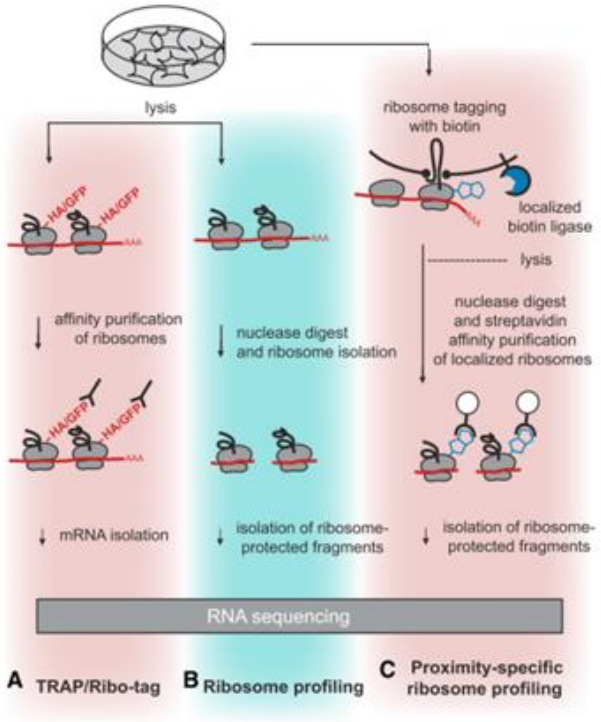

Figure 1.6 Overview of RNA-Seq based methods(Chekulaeva & Landthaler, 2016). A) Affinity tagged ribosomes are immunoprecipitated by specific antibodies, and mRNA isolation is done further. B) Translating mRNAs are pulled-down by affinity purification or sedimentation, ribosome-protected mRNA fragments are extricated by RNase treatment. C) Proximity-specific ribosome profiling, biotin-tagged ribosomes are pulled-down with affinity purification after nuclease digest.

1.2.2.1 Ribosome Profiling and Proximity-Specific Ribosome Profiling

Monitoring gene expression has focused on the measuring of mRNA level by relying on RNA-seq and microarray experiments. Besides, translational control and protein expression of genes are other aspects of gene expression regulation. There may not be a linear correlation between mRNA expression in certain cases, translating mRNA levels and protein levels. Ribosome profiling is a method that may explain such discrepancies. Ribosome profiling is a deep sequencing-based method providing a

translation measurement with ribosome-protected mRNA fragments (Brar & Weissman, 2015). Ribosome profiling starts with inhibition of translation to freeze ribosomes, cell lysis, and nuclease digestion to generate ribosome-protected fragments, which reveals ribosome position and then ribosome isolation process, which produces ribosome footprints. Polysome isolation can be applied with sucrose gradient sedimentation or with pull-down via ribosomal proteins (Sanz et al., 2009). Approximately 30 nucleotides (Gobet & Naef, 2017) ribosome footprints are inverted to a strand-specific library for next-generation sequencing. Next, ribosome footprint fragments are mapped to the appropriate reference genome (Ingolia, Brar, Rouskin, Mcgeachy, & Weissman, 2012).

Proximity Specific Ribosome Profiling enables analysis of translation in defined subcellular localization. Initially, this technique was applied to study cotranslational translocation into the endoplasmic reticulum (ER) in yeast. 80S ribosomes were tagged at C' terminus with biotin acceptor peptide TEV protease-cleavable AviTag via RPL16 and RPS2 proteins. Biotin ligase BirA were localized to the ER using the C-terminal tail-anchor (TA) from UBC6, SEC63, and SSH1 proteins embedded in ER. (Figure 1.7) (Jan, Jan, Williams, & Weissman, 2014). Pulldown of ER-specific ribosomes and then deep sequencing was managed with proximity-specific ribosome profiling.

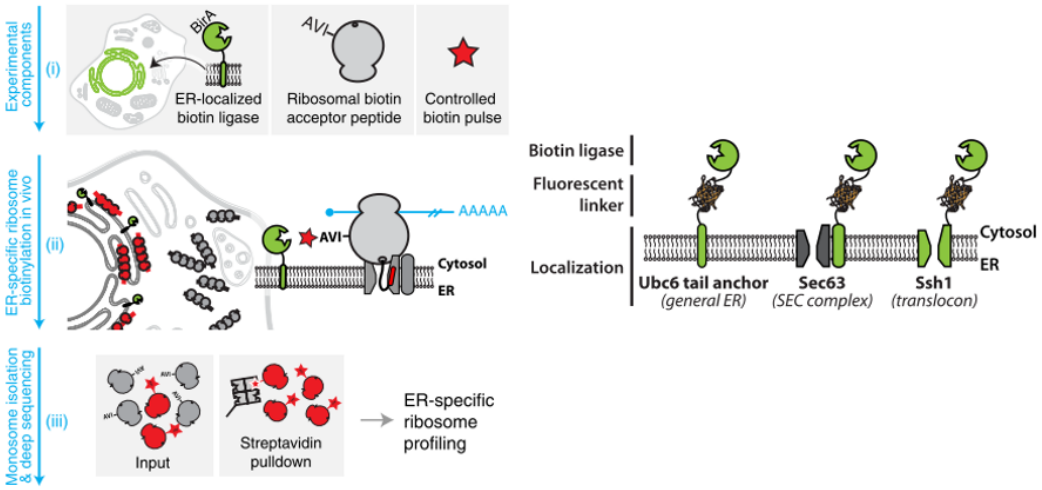

Figure 1.7 Proximity-Specific Ribosome Profiling on Endoplasmic Reticulum (Jan et al., 2014).

1.2.2.2 Translating Ribosomal Affinity Purification

Ribosomal affinity purification (RAP) or translating ribosomal affinity purification (TRAP) resembles ribosome profiling as cell lysis, and polysome pull-down with affinity tag is common in both techniques (Figure 1.8). In ribosome profiling, RNA is obtained as approximately 30 nucleotide ribosome footprints with nuclease treatment, and deep-sequencing is applied. Nevertheless, mRNAs are obtained in full length in the TRAP method because nuclease treatment is not applied, and RT-qPCR, microarray or RNA-seq can be used after RNA isolation.

TRAP was developed to generate a cell-type-specific translational profiles and rely on the isolation of mRNA populations which associate with the 80S ribosome. This method evaluates rapid and dynamic changes of mRNA association with ribosomes, which can be modulated in response to environmental signals (Alonso & Stepanova, 2015). For example, TRAP has been used to reveal translatome changes in response to cold stress, low oxygen availability, and pathogen infections in plants (Halbeisen, 2009; Halbeisen, Scherrer, & Gerber, 2009; Inada et al., 2017; Moeller et al., 2012;

Mustroph et al., 2009). This method combines a recombinant gene expression with affinity purification (Heiman, Kulicke, Fenster, Greengard, & Heintz, 2014). Recombinant protein is generated with the fusion of ribosomal protein and appropriate affinity tag. Large subunit proteins, RPL10A, RPL18 RPL22, or RPL25 are tagged with eGFP, HA, Flag, biotin, and polyhistidine from N-terminus. In most of the mammalian studies, eGFP-RPL10A fusion gene has been used.

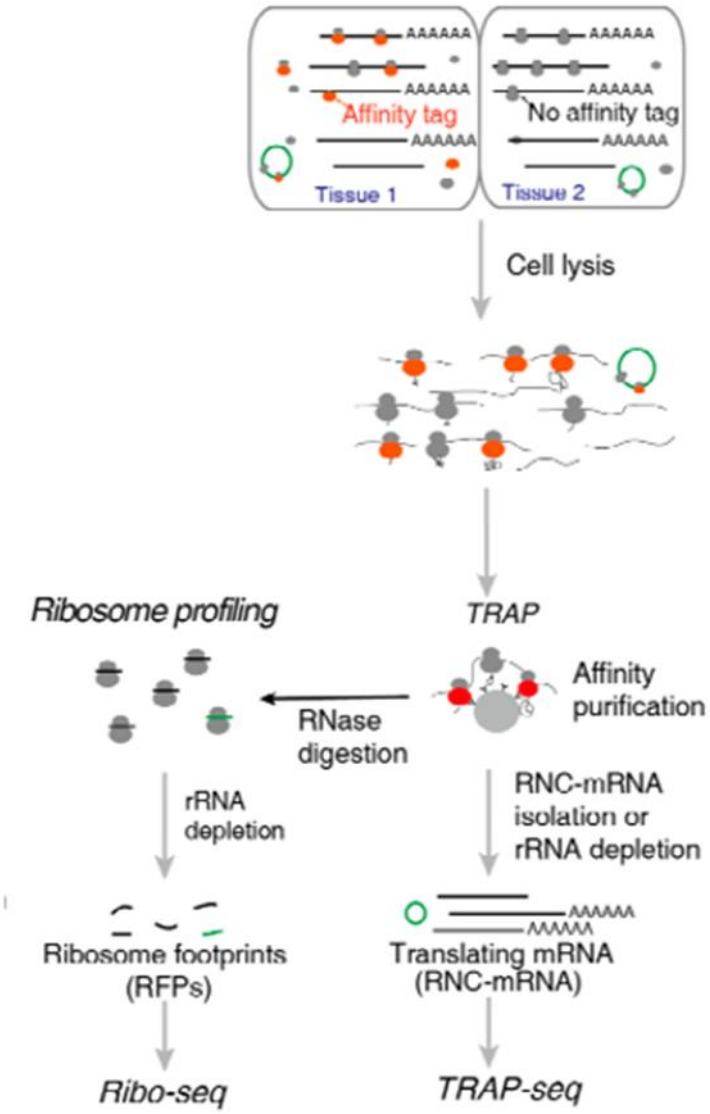

Figure 1.8 Ribosome Profiling and Translating Ribosomal Affinity Purification (TRAP)

The application of this method involves a series of steps. First of all, to freeze ribosomes in the act of translation, 100 µg/ml cycloheximide (CHX) treatment is applied to eGFP-RPL10A expressing cells. Cell lysis step is followed by affinity purification of ribosomes/polysomes with appropriate antibody or bead to the affinity tag. After pull-down of ribosomes, isolation of translating mRNAs is

performed with a kit or TriZol based RNA extraction method. Next, isolated mRNAs can be used in further gene expression analysis experiments such as northern blot, qPCR, microarray, and RNA-seq.

TRAP method has been used in different organisms, tissues, and cells, from mice to plants, neurons, yeast, Drosophila (Bertin, Renaud, Aradhya, Jagla, & Junion, 2015; X. Chen & Dickman, 2017; Morin, Daneman, Zavortink, & Chia, 2001), and Xenopus laevis retina (Watson, Mills, Wang, Guo, & Chen, 2012). Especially in mouse, TRAP is applied to different tissues including brain (Ainsley, Drane, Jacobs, Kittelberger, & Reijmers, 2014; Doyle et al., 2008; Heiman et al., 2008; E. F. Schmidt, Warner-schmidt, Otopalik, Pickett, & Greengard, 2012; Visanji & Sarvestani, 2015), and kidney (Liu et al., 2014). Expression of eGFP-RPL10A is shown in figure 1.4.

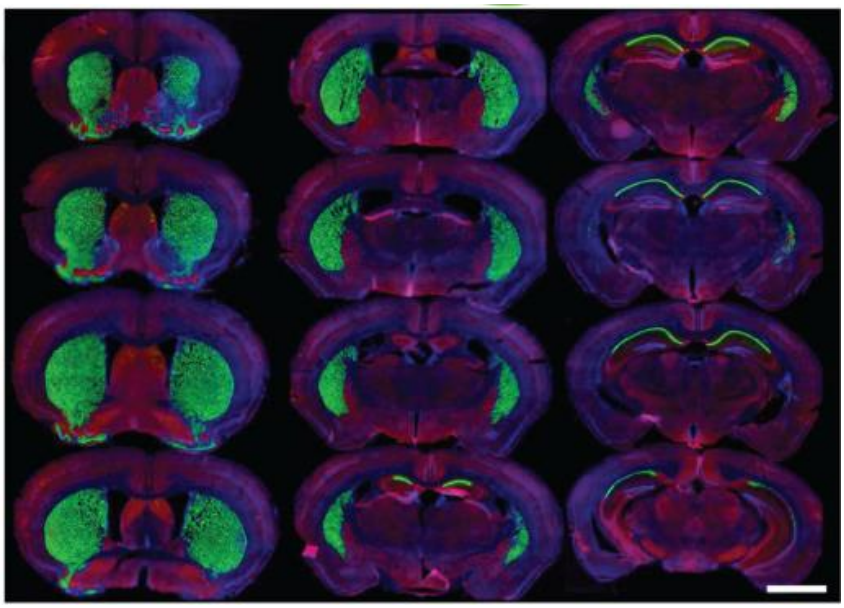

Figure 1.9 EGFP-L10a expression throughout the brain of a 3-month-old Camk2a-TRAP mouse. Green, EGFP-L10a; red, Gad1; blue, DAPI. Scale bar, 2 mm (Drane, Ainsley, Mayford, & Reijmers, 2014).

In *in vivo* studies, TRAP provides expression profile information in complex tissues such as the central nervous system (CNS). In conventional cell separation

techniques, mRNA degradation, disruption of tissue-specific intrinsic signaling, low expression of target mRNA, limited material, myelin, and blood contamination were problematic (Doyle et al., 2008). However, TRAP overcomes these problems with affinity purification and CHX treatment.

Alternative transcription start sites, alternative splicing, and alternative polyadenylation generate multiple mRNA transcripts with different translation rates and ribosome occupancy. TRAP method can reveal these differences and provides detection of the translational profile of genes (Dougherty, 2017).

In a mouse study, TRAP was combined with in utero electroporation (IUE) to study molecular profiles of specific neuronal populations during neonatal development. The neurons in the somatosensory cortex were targeted by TRAP, and approximately 7300 mRNAs translation change in differentiation was observed. (Gong, Zhang, Kim, & Matthew, 2018).

In another study, the TRAP method was applied from a different point. Biotinylation of Avi-EGFP-Rpl10a was used in the skeletal muscle of Danio rerio (zebrafish) to detect changes in translation of development-related mRNAs (Housley et al., 2014). Model organism zebrafish can regenerate cardiac tissue with proliferation of spared cardiomyocytes after injury. TRAP was used to profile translating mRNAs in cardiomyocytes during regeneration. Jak1/Stat3 pathway member's induction was observed (Fang et al., 2013).

TRAP method has been a useful tool in different plant studies (Wellmer, 2016). RPL18 was commonly used with His and Flag tag in Arabidopsis studies (Fernie & Schippers, 2012; Jiao & Meyerowitz, 2010; Juntawong & Bailey-serres, 2012; Mustroph et al., 2009). In another study, rice (Oryza sativa) was used for a TRAP-seq experiment, and the effect of GC content, transcript length, and transposable element content of mRNAs in translation was revealed (D. Zhao et al., 2017).

1.3 Multiple Isoforms From One Gene

Eukaryotic genes can generate RNA isoforms in a surprising variety through alternative splicing, alternative transcription start site, and alternative polyadenylation, which often cell type-specific (Floor, Doudna, States, & Initiative, 2016). Alternative transcription start site (TSS) leads to different RNA isoforms differing in their first exon or in the length of the 5' untranslated region (5'UTRs). The use of different first exon changes the open reading frame (ORF) and protein variety (Licatalosi & Darnell, n.d.).

TSS detection methods provide the diversity of transcriptional initiation events. For example, cap analysis gene expression (CAGE) method showed that alternative TSS is highly tissue-specific, and the number of alternative TSS is different in tissue types (Consortium, Pmi, & Dgt, 2014). Studies focusing on a single gene reveal that TSS selection is crucial in development, differentiation, disease progress such as cancer, neuropsychiatric, and development disorders (Hill, Lettice, & Hill, 2013; Pedersen et al., 2002; Pozner et al., 2007).

Differential inclusion of subsets of exons results in alternatively spliced gene transcripts. Alternative mRNA processing can result in different mRNA isoforms that encode a variety of proteins or alter untranslated regions (UTRs) that affect mRNA stability, translation, and localization. Besides, these alternative processes can generate non-functional RNA isoforms degraded in nonsense-mediated decay (NMD) to control the expression of a gene (Figure 1.6).

Most animal alternative splicing (AS) is regulated as tissue-specific. For example, brain, heart, and muscle show strong splicing signatures conserved between mammals and chicken, such as eukaryotic translation elongation factor 1 delta (EEF1d) (Merkin, 2012). In the nerveous system, AS has many crucial roles, including the expression of isoform that are essential for neurodevelopment (Ule & Darnell, 2006). For example, in *D. melanogaster*, *Dscam* (Down syndrome cell

adhesion molecule) can give rise to 38,016 neuron-specific RNA variants generated by AS (Hattori, Millard, Wojtowicz, & Zipursky, 2008).

In short, alternative splicing provides a transcript variety and regulates transcript abundance (Licatalosi & Darnell, 2010).

AS can also cause a coding frameshift, and this can lead to the formation of a premature termination codon (PTC). PTC induces degradation of the mRNA by the NMD pathway in coordination with the translating ribosomes. Deregulation of splicing has been associated with diseases such as cancer. Many splicing machinery mutations contribute to tumorigenesis. Dysregulated RNA splicing machinery causes the expression of cancer-specific isoforms in tumorigenesis states (Wang & Aifantis, 2020). In addition, alterations in splicing can lead to neoantigen formation in cancer patients (Kahles et al., 2018).

Alternative polyadenylation (APA), cleavage of 3' end, and addition of poly(A) tail in a pre-mRNA is a process that generates different 3'ends from the same gene. Almost all eukaryotic mRNAs and many non-coding RNAs (ncRNA) are polyadenylated, and many eukaryotic genes have more than one poly(A) (p(A)) site (Tian, Hu, Zhang, & Lutz, 2005). APA events can be examined in three groups. In the first group, there is only one poly(A) signal in 3'UTR that leads to one mRNA isoform and one type of protein. In the second group, there is more than one poly(A) signals in 3'UTR, and these signal sites lead to different poly(A) tail positions in mature mRNA. These two isoforms are different in point of 3'UTR lengths, and the same protein would be synthesized. However, the length of the 3'UTRs can change the mRNA half-life and translation efficiency because longer 3'UTRs can harbor more microRNA (miRNA) binding sites (Figure 1.6), and more RNA-binding protein (RNABP) recognition sites or can alter the RNA secondary structure (Erson-bensan & Can, 2016). In the third group, APA is coupled to AS, and poly(A) sites may exist in introns or exons. Thus, different proteins may be produced depending on the location of the stop codon (Akman & Erson-bensan, 2014).

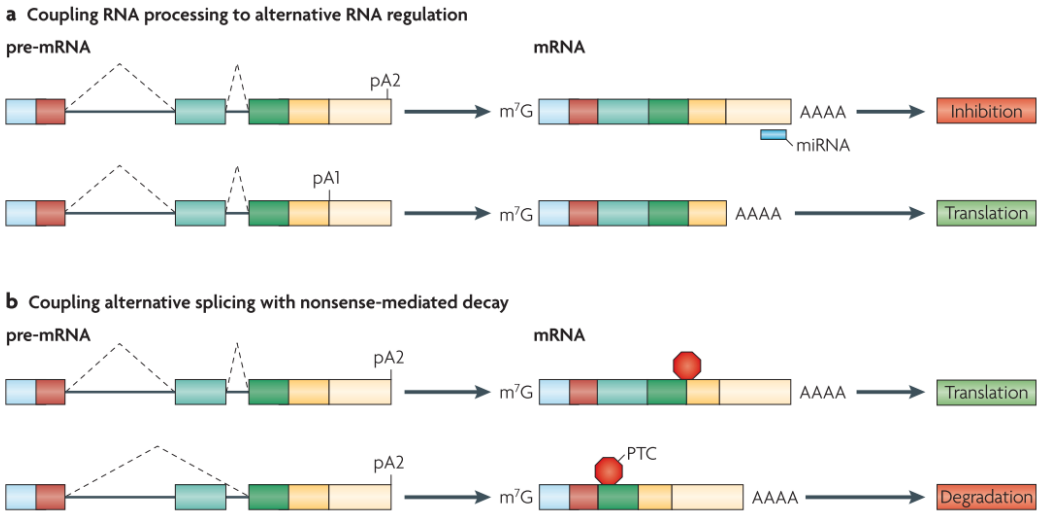

Figure 1.10 Coupling RNA processing to alternative RNA regulations a) Alternative polyadenylation (APA) and translation inhibition b) Alternative splicing and NMD (Licatalosi & Darnell, 2010).

3'UTR regulations are controlled in crucial processes such as development, cell programming, and cell homeostasis. 3' shortening or lengthening in mRNA poses different biological results. Short 3'UTR (proximal poly(A) site preference) has been associated with proliferation and transformation. Many oncogenes have been associated with 3' shortening in tumor cells (Chen et al., 2017). APA might be a mechanism by which oncogenes can escape from microRNA-mediated repression in cancers (Mayr & Bartel, 2009).On the other hand, long 3'UTR use (distal poly(A) site preference) is thought to be associated with development and differentiation (Akman & Erson-Bensan, 2014). Hence it is of great importance to study cancer-specific isoforms to better understand molecular mechanisms underlying cancer. To begin understanding the consequences of isoform diversity in cancers, studying coding potential and ribosome association is an important starting point in most molecular studies.

1.4 Aim of The Study

Translating ribosomal affinity purification (TRAP) is a useful technique to detect translating mRNAs *in vivo*. We aimed to optimize this method for in vitro use with high specificity magnetic bead conjugated Llama Anti-GFP VHH Single Domain Monoclonal Antibody (Magnetic Beads) (ABCAM, ab-193983) to pull down eGFP-RPL10a ribosomal protein as part of actively translating ribosomes. We were able to show ribosome association of coding mRNAs and lack of association with non-coding RNAs. This optimized model will be available for studying the ribosome association of RNAs.

CHAPTER 2

MATERIAL METHOD

2.1 Cell Lines and Cell Culture

HEK293 and MCF-7 cell lines were cultured in Dulbecco's Modified Eagles's Medium containing High Glucose (4500 mg/L Glucose), 1% penicillin-streptomycin, 10% Foetal Bovine Serum (FBS), 2 mM L-glutamine, 1.5 g/L sodium bicarbonate, and 1 mM sodium pyruvate. To prevent mycoplasma contamination, 25 mg/ml Plasmocin (Invitrogen, Cat#: ant-mmp) was added to culture medium. Cell lines were incubated at 37°C with 95% humidified air and 5% CO_2. For long-term cell storage, cell pellets were resuspended with medium including 5% DMSO (dimethyl sulfoxide) (Sigma, cat#: 154938)

2.2 Cloning of RPL10A Gene into pEGFP-C1 Vector

The coding sequence of the RPL10A gene was retrieved from NCBI (National Center for Biotechnology) with the accession number NM_007104.4. Specific forward and reverse primers that contain *BglII* and *HindIII* restriction recognition sites were designed for PCR amplification of the 676 nucleotide long full coding sequence of RPL10A. CGCAT random sequence was added to both 5'end of restriction sites to enhance digestion, shown in Table 2.2.1. For primer optimization, gradient PCR was performed. Gradient PCR reaction content and temperatures are indicated in Table 2.2.2.

Table 2.2.1 RPL10A Cloning Primers

Forward L10A Cloning Primer	5’CGCAT**AGATCT**ATGAGCAGCAAAGTCTC 3’
Reverse L10A Cloning Primer	5’CGCAT**AAGCTT**TTAATATAGGCGCTGGGGCT 3’

Table 2.2.2 Gradient PCR Reaction Mixture

1X PCR MIXTURE	
10X Taq Buffer	2 µl
2mM dNTPs	2 µl
5µm Forward Primer	2 µl
5µm Reverse Primer	2 µl
Template DNA	1 µl
Taq DNA Polymerase	0.2 µl
Molecular grade water (mgH_2O)	9.2 µl
Annealing Temperatures	56 °C, 56.7 °C, 57.9 °C, 59.8 °C, 62.1 °C, 64.0 °C, 65.3 °C, 66.0 °C

Table 2.2.3 Amplification of RPL10A with Phusion High Fidelity Polymerase

1X PCR Mixture	
5X Phusion High Fidelity Buffer	10µl
Forward Cloning Primer	5 µl
Reverse Cloning Primer	5 µl
2 mM dNTPs	5 µl
Template DNA	2.5 µl
Phusion High Fidelity Polymerase (2U/ µl)	0.5 µl
Molecular grade water (mgH_2O)	22 µl

64°C was used for annealing step of PCR using primers for RPL10A cloning into EGFP-C1 vector (a kind gift from Prof. Dr. Volkan Seyrantepe). The resulting vector is shown in the APPENDIX B section.

For amplification of the desired gene, PCR was performed with Phusion-High Fidelity DNA polymerase (F530L, Thermo Fisher Scientific) and the conditions for amplification were as follows: initial denaturation at 98°C for 3 minutes; 35 cycles of 98°C 30 seconds, 64°C for 30 seconds, 72°C for 30 seconds, and final extension 72°C for 5 minutes. Table 2.2.3 mixture of PCR.

PCR products were run on 1% agarose gel, and the band of the expected size was cut from the gel, to purify the DNA using the Zymoclean Gel DNA Recovery Kit (D40008, Zymo Research). pEGFP-C1 empty vector and isolated DNA product were quantified with NanoDrop (MN-913, Maestrogen). PCR product and empty pEGFP-C1 vector (5000ng) were double digested with Bgl II and Hind III fast digest

restriction enzymes for 1 hour at 37°C. The calculation and mixture for vector and PCR product is shown with the following formula and Table 2.2.4.

$$\frac{vector\ amount(ng)}{vector\ concentration(ng/\mu l)} = vector\ volume(\mu l)$$

$$\frac{5000ng}{395.05ng/\mu l} = 12.65\ \approx 13\ \mu l$$

Table 2.2.3 Double Digestion Reaction Mixtures

Double Digestion	Insert	Vector
mgH_2O	23 µl	30 µl
10x Fast Digest Buffer	5 µl	5 µl
Bgl II	1 µl	1 µl
Hind III	1 µl	1 µl
DNA	20 µl	13 µl

Double Digestion mixtures were incubated for 1 hour at 37°C. After digestion, uncut and cut pEGFP-C1 vectors were run for control on 1% agarose gel.

The digested pEGFP-C1 vector and Insert were mixed and ligated by using T4 DNA Ligase enzyme (EL0011, Thermo Fisher Scientific). Calculations for ligation were carried out according to the following formula:

Required vector quantity:

$$\frac{vector\ amount(ng)}{vector\ concentration(ng/\mu l)} = vector\ volume(\mu l)$$

Required insert quantity:

$$Insert\ mass = \frac{vector\ mass\ x\ insert\ weight}{vector\ molecular\ weight} x\ \frac{5}{1}$$

$$\frac{200ng\ x\ 0.6767\ x\ 5}{4.731} = 142.89\ ng$$

Required insert volume:

$$Insert\ volume = \frac{mass\ (ng)}{concentration\ (ng/\mu l)}$$

$$\frac{142.89\ ng}{100.97\ \ ng/\mu l} = 1.4\ \mu l\ insert\ volume$$

Table 2.2.4 Ligation Reaction Components

	No insert	Insert
mgH_2O	7.4 µl	6 µl
Vector	1.4 µl	1.4 µl
Insert	-	1.4 µl
T4 DNA Ligase Enzyme	0.2 µl	0.2 µl
T4 DNA Ligase Buffer	1 µl	1 µl

2.2.1 Transformation of Competent *E.coli* TOP10 Strain

50 µl competent TOP 10 *E.coli* cells were thawed on ice and then mixed with 3 µl ligation product and incubated on ice for 30 minutes. After incubation, heat shock was performed at 42°C for 1 minute, the cells incubated on ice for 5 minutes. 500 µl Nutrient Broth (NB) medium was added on mixture and incubated at 37°C for 60-90 minutes. Nutrient Broth agar plated were prepared with 100 µl/ml kanamycin. After incubation, centrifugation was performed at 3000 rpm, 25°C for 5 minutes. 400 µl of supernatant was removed, and the pellet was mixed with remaining NB by pipetting. 100 µl of transformed bacteria inoculated to NB agar plate and incubated at 37°C overnight.

Colony PCR was performed to confirm positive colonies for pEGFP-C1_RPL10A vector. Selected positive colonies were inoculated in NB media at 37°C overnight with 180 rpm. Then, plasmids were isolated with K0503 GeneJET Plasmid Miniprep Kit 250RXN kit according to the instructions of the manufacturer.

2.3 Stable Transfection of HEK293 and MCF-7 Cell Lines

HEK293 and MCF-7 cells were seeded on 6-well plates and incubated at 37°C with 95% humidified air and 5% CO_2. After the cells reached 70-80% confluency, transfection was done with TurboFect Transfection Reagent (R0532, Thermo Fisher Scientific). In a 1.5 ml centrifuge tube, 400 µl DMEM and 2 µg plasmid were mixed by gentle pipetting. Then, 8 µl TurboFect (Thermo Fisher Scientific, R0532) was added and mixed by pipetting and incubated for 30 minutes. After incubation, the solution was added to the cells. To generate stable cell lines, 24 hours after transfection, medium with G418 (Roche, REF 04727878001 20 mL POTENCY 892 ug/mg) was added for selection. For HEK293 cell line, the medium contained 500 µg/ml G418, MCF-7 cell line medium contained 800 µg/ml G418. After two weeks,

polyclonal stable transfected cells were obtained, and G418 concentration was decreased 50% for both cell lines.

2.4 Sorting of eGFP-L10A Expressing HEK293 and MCF-7 Cell lines

GFP-RPL10A overexpressing cells were generated for both HEK293 and MCF-7 cell lines with stable transfection, as mentioned in Section 2.4. To obtain the highest GFP-RPL10A expressing cells, polyclonal cell lines were sorted with BD FACSMelody in CanSyL by Dr.Deniz Cansen Kahraman. After the sorting process, cells were seeded on the 6-well plates. After two days, cells were passaged to T-75 flasks.

2.5 Western Blot

2.5.1 Protein Isolation

Total proteins were isolated with M-PER Mammalian Protein Extraction Reagent (Thermo, Cat#: 78501). Protein isolation was performed according to manufacturers' protocol. Protease inhibitor (Roche, Cat#: 1187350001) and PhosSTOP (Roche, Cat#: 04906837001) were added to M-PER reagent to prevent protein phosphorylation and degradation. protein concentrations were measured using Pierce Protein Assay Kit (Thermo, Cat#: 23227). Isolated proteins were stored at -80°C freezer.

2.5.2 Western Blotting and Antibodies

50 µg of protein was boiled in 6X Laemmli Buffer at 95°C for 10 minutes and then loaded to 10% SDS-polyacrylamide gel. Protein separation was performed at 100 V for 1 h. After separation, the transfer of proteins onto PVDF membrane (Merck, cat#:

03010040001) was performed. For blocking of the membrane, skim-milk (Bio-Rad Blotting-Grade Blocker, cat#:170-6404) was used in 0.5% TBS-T buffer. Membrane was incubated in 5% skim-milk and 1:500 anti-GFP mouse primary antibody(Santa Cruz, sc-9996) overnight at 4°C and 1 hour at room temperature with 5% skim-milk and 1:3000 HRP-conjugated goat-anti mouse secondary antibody. For the visualization of the membrane, WesternBright ECL (Advansta, cat#: K12045-D50) reagent, Chemidoc MP imaging system, and Odyssey Classic Imager (LI-COR) were used.

2.6 Immunoprecipitation of eGFP-RPL10A fusion protein with Anti-GFP VHH Single Domain Antibody (Magnetic Beads) (ABCAM, ab-193983)

Immunoprecipitation was performed to test the specifity of the magnetic bead conjugated Llama Anti-GFP VHH Single Domain Monoclonal Antibody (Magnetic Beads) (ABCAM, ab-193983). HEK293 cells grown on a T75 flask were lysed with a lysis buffer that contains 150 mM NaCl, 10 mM Tris-HCl (pH 7.4), 1 mM EDTA, 1% Tripton X-100, 0.5% NP-40, 1X phosSTOP, 1X protease inhibitor by incubating on ice for 30 minutes with pipeting every 10 minutes. Next, the lysate was collected with centrifugation at 20.000 g for 10 minutes at 4°C.

Magnetic beads (Anti-GFP VHH Single Domain Antibody, ABCAM, ab-193983) were equilibrated with wash/dilution buffer that contains 150 mM NaCl, 10 mM Tris-HCl (pH 7.4), 1X phosSTOP, 1X protease inhibitor. Lysate and equilibrated beads were mixed by pipetting and then incubated for 1 hour at 4°C. After incubation, the supernatant was collected using a magnetic rack and transferred to a new microcentrifuge tube. Bead-protein complexes were washed 3 times with the wash/dilution buffer. After washing, buffer was removed, and bead-protein complexes were boiled with 100 µl 2x SDS-laemmli buffer. Boiled proteins were

separated from beads via magnetic rack. Obtained proteins were run in 10% SDS-polyacrylamide gel and all blotting process was performed as per section 2.5.2.

2.7 Translating Ribosomal Affinity Purification (TRAP)

2.7.1 Cell Culture

eGFP (EV) (Empty pEGFP-C1 vector) and eGFP-RPL10A (pEGFP-C1_RPL10A) expressing HEK293 cell lines were used for TRAP. eGFP (EV) (Empty pEGFP-C1 vector) cells were used for immunoprecipitation negative control. The medium of all EV and eGFP-RPL10A flasks was aspirated, and 8 ml of growth medium with 100 µg/ml Cycloheximide (CHX) was added. Cells were incubated for 15 minutes at 37°C with 95% humidified air and 5% CO2. After incubation, the medium was aspirated, and the cells were washed with ice-cold PBS with 100 µg/ml CHX. The cells were scraped with PBS-CHX. Cell pellet was collected with centrifugation at 1500 g for 5 minutes at 4°C.

2.7.2 Cell Lysis

Collected pellets were lysed with lysis buffer (10 mM Tris-HCl pH 7.5, 150 mM NaCl, 100 mM $MgCl_2$, 1X phosSTOP, 1X protease inhibitor, 100µ/ml CHX, 0.5% NP-40 (10%), 0.5 mM ditiotreitol (DTT), 40 unit Superasin (Applied Biosystems cat#: AM2694) 40 unit rRNAsin (PROMEGA N2511 Recombinant RNasin Ribonuclease 2500 unit)).

2.7.3 Polysome Immunoprecipitation

Magnetic bead conjugated llama Anti-GFP VHH single domain monoclonal antibody (magnetic beads) (ABCAM, ab-193983) was equilibrated (washed) with

wash buffer that contains 10 mM Tris-HCl pH 7.5, 150 mM NaCl, 100 mM $MgCl_2$, 1X phosSTOP, 1X protease inhibitor, 100µ/ml CHX, 0.5 mM ditiotreitol (DTT). Equilibrated (washed) magnetic beads were mixed with lysate and incubated at 4°C for 16-18 hours by rotating. Next day, the supernatant was separated from bead-polysome complexes with the magnetic rack, and the washing step was performed twice. After washing, 500 µl TriZol was added to magnetic bead-polysome complexes, and pipetting was performed extensively. The solution was separated from magnetic beads with magnetic rack. Next, RNA isolation process was performed as outlined in section 2.8.

2.8 RNA Isolation and DNase I Treatment

RNA Isolation was performed with Phenol-Chloroform with TriZol Reagent (Invitrogen, CAT#: 15596-018). After the addition of Trizol, samples were incubated at room temperature for 5 minutes. Then 100 µl chloroform (Applichem, APA3691.1000) was added and incubated on ice for 15 minutes and then centrifuged at 12,000 g at 4°C for 15 minutes. Upper phase of the solution was transferred to a new minicentrifuge tube and mixed with 250 µl isopropanol. Next, mixtures were centrifuged at 12,000 g at 4°C for 15 minutes. RNA pellets which were collected by centrifugation were washed with 75% molecular grade ethanol with re-centrifuge at 12,000 g at 4°C for 15 minutes. Samples were air dried to eliminate excess ethanol from RNA pellet. Next, RNA pellets were resuspended in 30 µl molecular grade H_2O.

After RNA isolation, *GAPDH* PCR control was done to check genomic DNA contamination with *GAPDH* forward and reverse primers. In cases of DNA contamination in samples, 2.5 µl (25 Unit) DNase I enzyme (Roche, cat#: 04716728001) treatment was performed for 1 hour at 37°C. Then, 100 µl Phenol: Chloroform: Isoamyl Alcohol (25:24:1) (pH4) was added to the DNase I treatment

reaction tube to stop the reaction. Mixtures were incubated on ice for 15 minutes and then centrifuged at 12,000 g at 4°C for 15. Next, the upper phase was mixed with 3 M sodium acetate and 100% molecular grade ethanol and then incubated -20°C overnight. Next day, centrifugation was performed at 12,000 g at 4°C for 30 minutes.Then RNA pellets were washed with 70% ethanol. Air dry was performed to eliminate excess ethanol from RNA pellet. Next, RNA pellets were solved in 30 µl mgH2O.

Then, to check DNA contamination, again, *GAPDH* PCR was performed with the same primers. Collected RNA was measured with NanoDrop (MAESTROGEN). Concentration, A260/A230, and A260/A230 ratios of RNA were checked for further use.

2.9 cDNA Synthesis

500 ng cDNA was synthesized from TRAP RNA by using RevertAid First Strand cDNA synthesis Kit (Thermo Fisher Scientific, Cat#: EP0441). Syhthesis of cDNA was performed according to the manufacturer's recommendations as shown in Table 2.9.1.

Table 2.9.1 cDNA synthesis Protocol

RNA	500 ng
Oligo(dT) primer (100µM)	1 µl
Nuclease-free water	1 µl
Incubation at 70°C for 5 minutes, after a short spin-down. Incubate on ice for 1 minute.	

5X Reaction Buffer (250 mM Tris-HCl (pH 8.3), 250 mM KCl, 20 mM $MgCl_2$, 50 mM DTT)	4 µl
dNTP mix (10 mM)	2 µl
RiboLock RNase Inhibitor (20 U/ µl)	1 µl
RevertAid Reverse Transcriptase (200 U/ µl)	1 µl
Incubation at 42 °C for 60 minutes, then heating up to 70 °C for 5 minutes.	

2.10 RT-qPCR

Real-Time Quantitative PCR (RT-qPCR) was performed using the QIAGEN Rotor-Gene Q Series detection system. BioRAD SYBR Green Supermix (Cat#: 172-5270), Ct values of reactions were calculated using the relative standard curves, and normalization for each reaction was made by using Ct values of the reference house-keeping gene RPLP0. Ct values were used to calculate ΔΔCq fold change (Bustin, 2009).

Table 2.10.1 All Primer Sequences

Name	**Sequence (5' to 3')** **Top: Forward Primer** **Bottom: Reverse Primer**	**Experiment**
L10a Cloning	CGCATAGATCTATGAGCAGCAAAGTCTC CGCATAAGCTTTTAATATAGGCGCTGGGGCT	Cloning
pEGFP-C1_L10a	AGCAAAGACCCCAACGAGAA GGGAGGTGTGGGAGGTTTTT	Sequencing
GAPDH	GGGAGCCAAAAGGGTCATCA TTTCTAGACGGCAGGTCAGGT	PCR
RPLP0	GGAAAAAGGAGGTCTTCTGG GGAAAAAGGAGGTCTTCTGG	RT-qPCR
HNRNPA1 Isoform 1	CAGAAGCTCTGGCCCCTATG CAGAAGCTCTGGCCCCTATG	RT-qPCR
HNRNPA1 Isoform 2&3	AAGTGTAAAGCATTCCAACAAAGG TCAGCGTCACGATCAGACCTG	RT-qPCR
HNRNPA1 Isoform 3	CAACCTGCTTGGGTGGAGAAA TTGCATAGGATGTGCCAACAA	RT-qPCR
XIST	TTACTCTCTCGGGGCTGGAA GGAGGACGTGTCAAGAAGACA	RT-qPCR
MALAT1_2	CAGCTCTGTGGTGTGGGATT TTGCAGGGACGGTTGAGAAG	RT-qPCR

CHAPTER 3

RESULTS

3.1 Expression of eGFP-RPL10A

3.1.1 Cloning of RPL10A into pEGFP-C1 vector

pEGFP-C1-RPL10A cloning was performed with RPL10A specific cloning primers given in CHAPTER 2, Table 2.10.1. The constructed coding sequence is shown in Figure 3.1

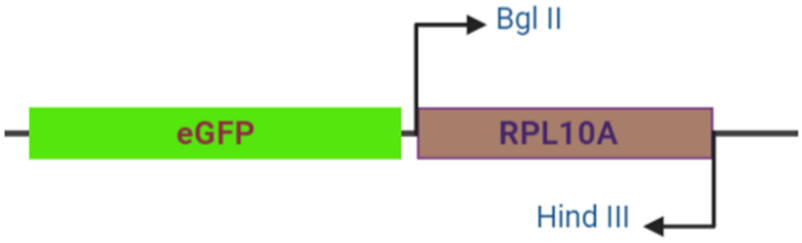

Figure 3.1 Cloning RPL10A coding sequence into pEGFP-C1 vector to synthesize RPL10A N-terminal fusion with eGFP

Colony PCR was used to screen bacterial colonies to test whether they had been transformed with pEGFP-C1 EV or pEGFP-C1_RPL10A constructs. After colony PCR, we picked a positive clone and cultured it. Next, plasmid isolation was performed, and pEGFP-C1_RPL10A plasmid was sent to sequencing with primers; sequences were given in TABLE Primers. Sequence results are shown in the APPENDIX C section.

3.1.2 Expression of eGFP-RPL10A Fusion Protein In Cell Lines

To optimize TRAP methodology, we used HEK293 and MCF-7 cell lines. After transfection of cell lines, I checked eGFP (EV), and eGFP-RPL10A (pEGFP-C1_RPL10A) expression with western blot and fluorescent microscopy (Floid) as shown in Figure 3.2.

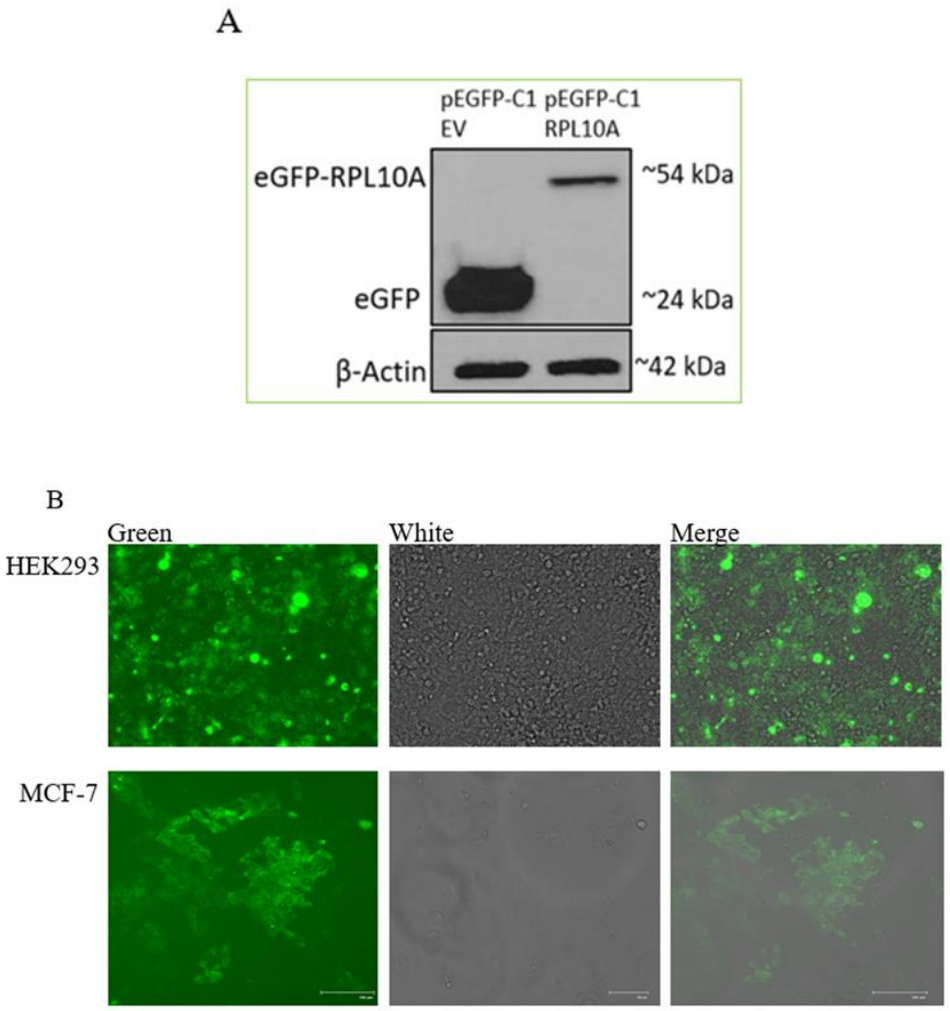

Figure 3.2 eGFP-RPL10A expression in transiently transfected HEK293 and MCF-7 cell lines. (A) eGFP and eGFP-RPL10A expression in HEK293 cell line, isolated proteins (50 µg) were loaded to 10% SDS-polyacrylamide gel GFP Ab: SantaCruz, sc-9996, (1:500 dilution in 0.5 %TBST with 5% skim-milk). ACTB (β-Actin) Ab: SantaCruz, sc47778 1:4000 dilution in 0.5% TBST and 3% skim-

milk. (B) eGFP-RPL10A expressing cells were observed with Floid under 20X magnification.

According to the western blot result (Figure 3.3A), transfection was successful, and the expression of fusion eGFP-RPL10A was confirmed.

3.1.3 Cell Sorting

Stable cell lines had heterogeneous populations expressing fusion protein at different levels. Low eGFP-RPL10A expressing cells in the populations could reduce the efficiency of immunoprecipitation experiments. Because of this, we aimed to obtain the highest eGFP-RPL10A cells. Cells were sorted using the BD FACSMelody. Plots of cell sorting for HEK293 is shown in Figure 3.3.

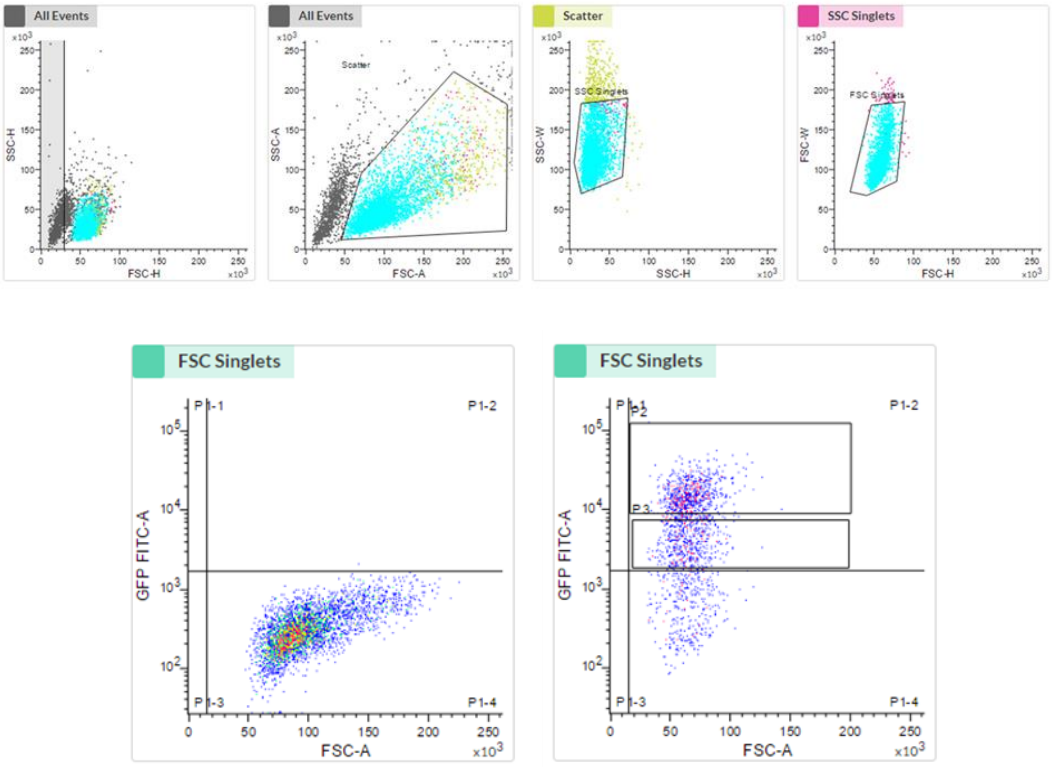

Figure 3.3 GFP expressing cell sorting. Approximately 5x10^6 cells were sorted for GFP expression. Forward Scatter (FSC) and Side Scatter (SSC) values were used for gating strategy. All Events SSC-H/FSC-H plot shows an adjusted threshold that discards debris according to Height (H). Similarly, All Events SSC-A/FSC-A plot grouped the cells for Area (A). Doublet discrimination was provided with first Scatter SSC-H (Height) / SSC-W (Widht) and then SSC Singlets FSC-H (Height) / FSC-W (Widht) plots. After gating, cells were grouped according to GFP expression.

FSC Singlets FSC-A / GFP FITC-A plot (Right one in Figure 3.4.B) shows GFP signal level of cells. In this plot, we determined two groups as P2 and P3 above the threshold. P2 indicates High GFP-RPL10A expressing cells, P3 indicates Low GFP-RPL10A expressing cells. GFP cell sorting was managed successfully, and the efficiency of the process was approximately 80% due to high transfection efficiency. Statistics of GFP cell sorting are shown in the APPENDIX D.

High GFP and Low GFP expressing cells were further confirmed by western blotting using the anti-GFP antibody (Figure 3.4).

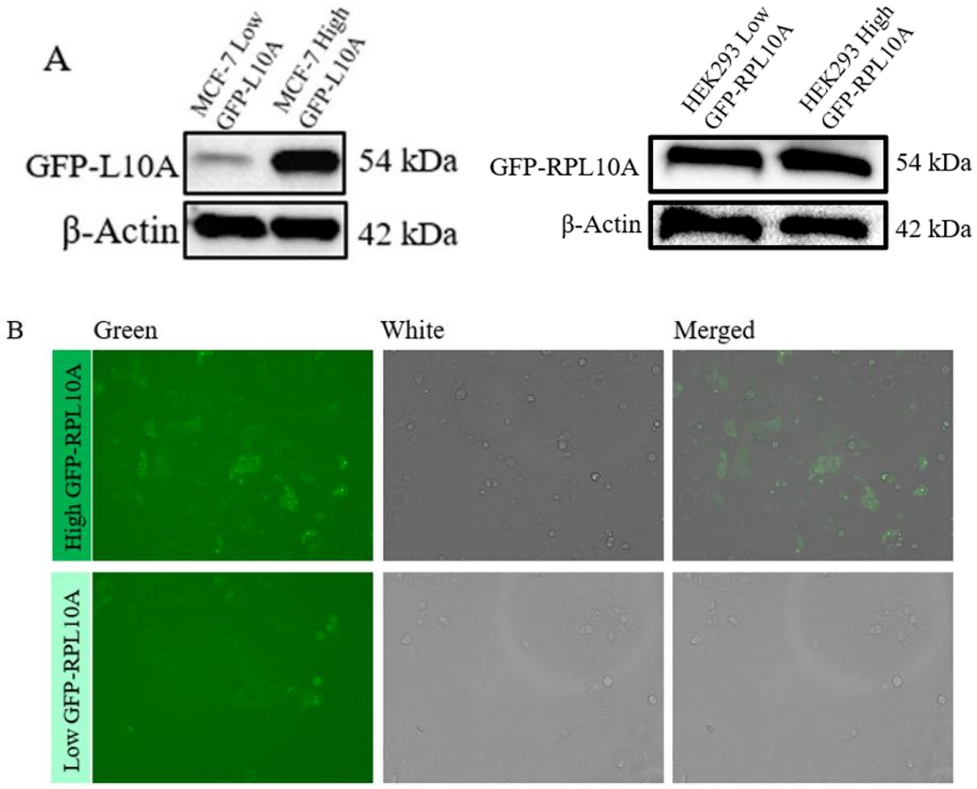

Figure 3.4 High and Low eGFP-L10A expressions. (A) 50 µg protein was used for western blotting in both HEK293 and MCF-7 cell lines. GFP Ab: SantaCruz, sc-9996, 1:500 dilution was prepared in 0.5 %TBST with 5% skim-milk. ACTB (β-Actin) Ab: SantaCruz, sc47778 1:4000 dilution was prepared with 0.5% TBST and 3% skim-milk. B) High and Low eGFP-RPL10A expressing MCF-7 cells were observed with Floid under 20X magnification.

3.2 Immunoprecipitation (IP) with Anti-GFP VHH Single Domain Antibody (Magnetic Beads) (ABCAM, ab-193983)

Optimization of Translating Ribosomal Affinity Purification (TRAP) includes crucial steps, and one of them is immunoprecipitation of ribosomes and polyribosomes. We chose magnetic beads conjugated Anti-GFP VHH single domain monoclonal llama antibody (sdAb) (magnetic beads) (ABCAM, ab-193983) to improve specific immunoprecipitation of ribosomes and polysomes.

To test whether immunoprecipitation was successful with Anti-GFP VHH single domain antibody (magnetic beads) or not, we performed an immunoprecipitation experiment with eGFP-RPL10A expressing HEK293 cells. The result of IP is shown in Figure 3.5.

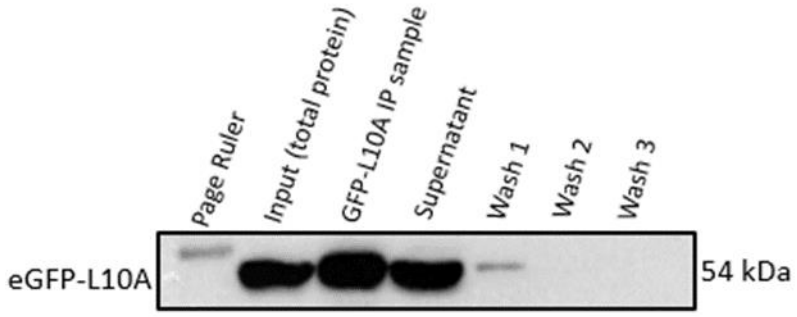

Figure 3.5 Control immunoprecipitation of eGFP-RPL10A in HEK293 cells. Immunoprecipitation was performed with Anti-GFP VHH Single Domain Antibody (Magnetic Beads) (ABCAM, ab-193983). 1000 µg of immunoprecipitated protein was loaded to 10% SDS-polyacrylamide gel and then transferred to the PVDF membrane. GFP Ab: Santa Cruz, sc-9996, 1:500 dilution was prepared in 0.5 %TBST with 5% skim-milk.

eGFP-RPL10A fusion protein was immunoprecipitated, as shown in Figure 3.5. Wash fractions were clear in immunoprecipitation, and this indicated washing steps were successful in eliminating non-specific binding.

3.3 Optimization of TRAP Method

3.3.1 Immunoprecipitation of Ribosomes

To prevent ribosome disassociation, we used high molarity of $MgCl_2$ (100 mM) (Nierhaus, 2014). Cycloheximide (CHX) concentration was 100 µg/ml for buffers and treatment (Heimann, 2014).

We always used cell cultures with 70-80% confluency to capture maximum translation level in cells. In the first experiment, we started only one T-75 flask of HEK293 cells equal to approximately $1x10^6$ cells. We obtained 28.63 ng/µl RNA in 30 µl mgH_2O with 50 µl anti-GFP VHH single domain magnetic beads. The bead amount was higher than the manufacturer's recommendation (20 µl). Because of this, we increased the cell number and used 5 T-75 (approximately $5x10^6$ cells) of EV and eGFP-RPL10A expressing HEK293 cells. Eventually, I performed three independent TRAP experiments. EV and eGFP-RPL10A RNA values are given in Table 3.1

Table 3.1 RNA concentrations of three TRAP replicates

	EV (ng/µl)	eGFP-RPL10A Before DNase I treatment (ng/µl)	eGFP-RPL10A After DNase I treatment (ng/µl)
TRAP 1	72	272.98	131.57
TRAP 2	68.1	298.82	130.90
TRAP 3	7.35	189.05	118.75

We used eGFP (pEGFP-C1 empty vector (EV)) expressing cells as a negative control for immunoprecipitation. We did not expect a pull-down of RNA in EV because eGFP (EV) does not incorporate the ribosome's structure. We saw expected results for EV, and in every TRAP experiment, EV RNA concentration was lower than the eGFP-RPL10A TRAP RNA (Table 3.1).

3.3.2 TRAP RNA In Further Experiments

3.3.2.1 Control PCRs and DNase I Treatment

We used phenol-chloroform extraction method with TriZol Reagent (Invitrogen, CAT#: 15596-018). After RNA isolation, we checked genomic DNA (gDNA) contamination by performing conventional PCR with *GAPDH* forward and reverse primers. In the case of gDNA contamination in the TRAP RNA sample, we performed DNAse I (25 Unit, Roche, cat#: 04716728001) treatment for 1 hour. Then, we rechecked RNA with GAPDH PCR. Then, we synthesized cDNA from at least 500 ng of TRAP RNA with oligodT primers. To check cDNA synthesis, we carried on GAPDH specific PCR. PCR results are shown in Figure 3.6.

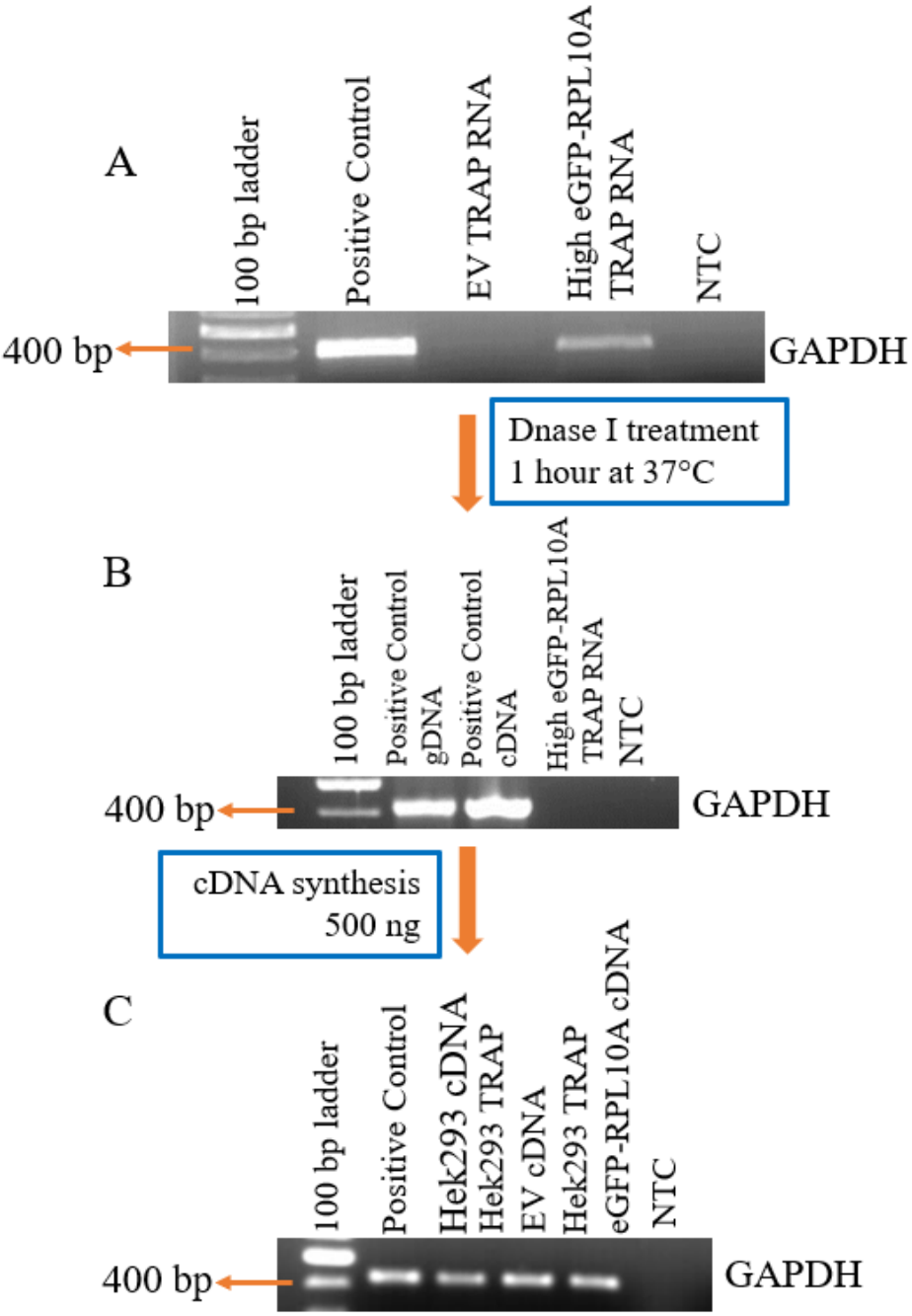

Figure 3.6 GAPDH PCRs A) gDNA contamination control, B) gDNA contamination control after DNase I treatment, C) cDNA synthesis control. High eGFP-RPL10A TRAP RNA was treated with DNase I for 1 hour at 37°C, then cDNA was synthesized, and then control PCR for GAPDH was performed.

3.3.2.2 Control PCRs and DNase I Treatment

To ensure specific IP of ribosome assocated mRNAs, we tested long noncoding RNAs (lncRNA). First, we used MALAT1 (NR_144567.1) gene as a negative control. However, Ct values of MALAT1 RT-qPCR were not useable due to low expression of the gene. We performed conventional PCR instead of RT-qPCR (Figure 3.7).

We then determined XIST (NR_001564.2) lncRNA as a negative control and performed RT-qPCR shown in Figure 3.7. In RT-qPCR, Hek293 TRAP cDNA was normalized to untransfected HEK293 cell line cDNA. TRAP-RNA samples were normalized to untransfected samples to determine whether TRAP-RNA samples were enriched or depleted of a specific transcript based on how much they are expressed in untransfected cells.

RPLP0 was used as a housekeeping reference gene. Ct values of every reaction were normalized to RPLP0.

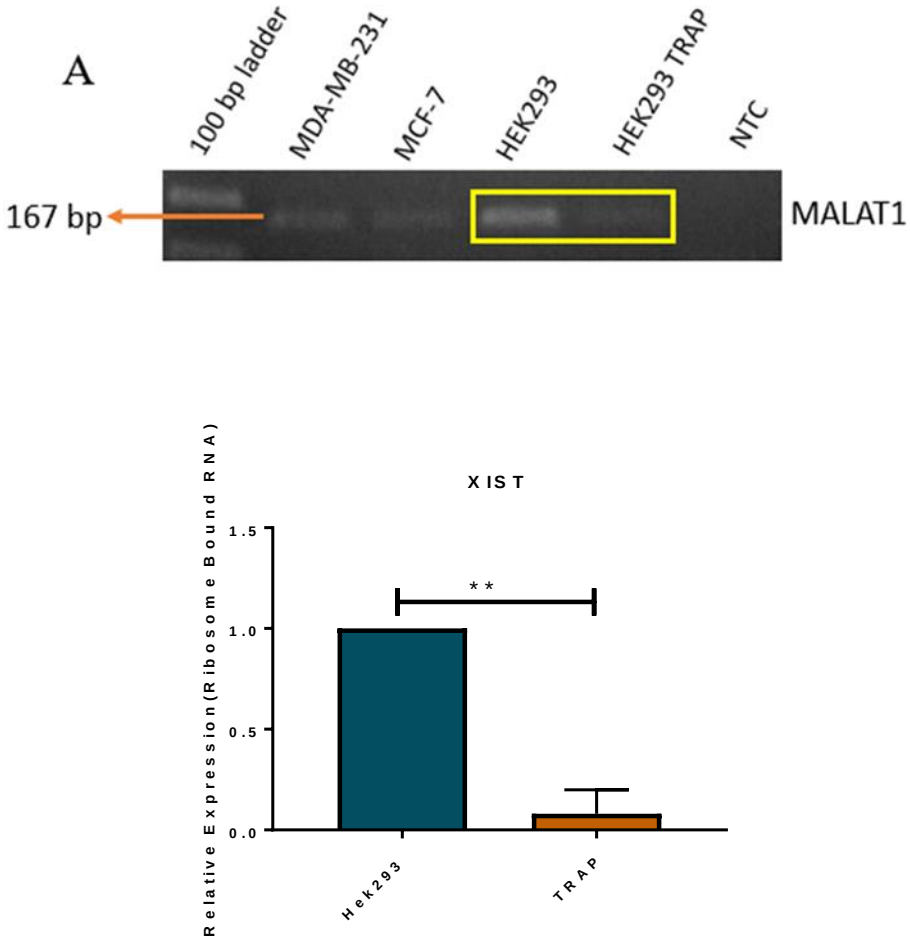

Figure 3.7 lncRNAs as a negative control. (A) conventional PCR with MALAT1 specific primers (35 cycles, annealing temperature is 65°C); product length 167 bp. Samples are untransfected HEK293 cell line cDNA and HEK293 TRAP cDNA. (B) RT-qPCR of XIST transcript. XIST expression level was normalized to that of untransfected HEK293 cell line. N=3 IP, every RT-PCR contains three technical replicates. Welch's t test was applied, p=0.0055 (**)

As expected MALAT1 was by lower in HEK293 TRAP than HEK293. XIST was low in the TRAP sample, indicating a significantly low association with the ribosome HEK293 RNA was higher 5-fold than TRAP RNA. These results suggested that we may have pulled down only translated mRNAs and not non-coding RNAs.

3.3.2.3 Testing ribosome association of transcript isoforms

For an ongoing project in the laboratory, we were interested in transcript isoforms of HNRNPA1 gene. According to NCBI, one of the isoforms (NR_135167, ENST00000547566.5) is indicated as a non-coding transcript. However, this transcript's coding sequence is identical to that of other isoforms, ENST00000330752.12, and ENST00000546500.5. Therefore it was important to test whether this isoform (NR_135167, ENST00000547566.5) is associated with polysomes. Figure 3.8 shows mRNA structures of HNRNPA1 Isoform 1, Isoform 2, and Isoform 3.

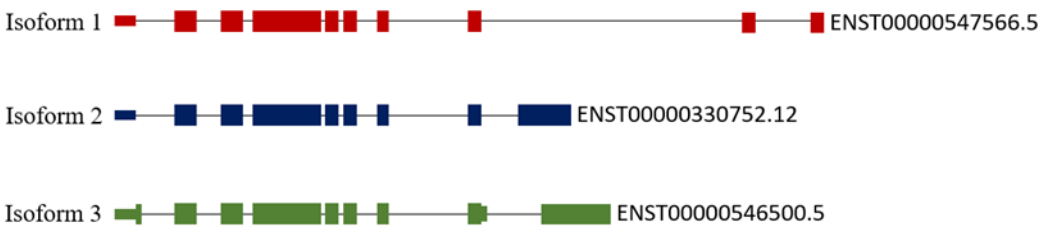

Figure 3.8 HNRNPA1 isoforms, Isoform1, Isoform2, and Isoform 3, Isoform 1 is indicated as non-coding isoform (NR_135167).

Following TRAP, we performed RT-qPCRs for three isoforms of HNRNPA1 using TRAP-cDNA. We normalized TRAP cDNA to untransfected HEK293 cDNA. The experiment was repeated three independent times (three immunoprecipitations of polysomes).

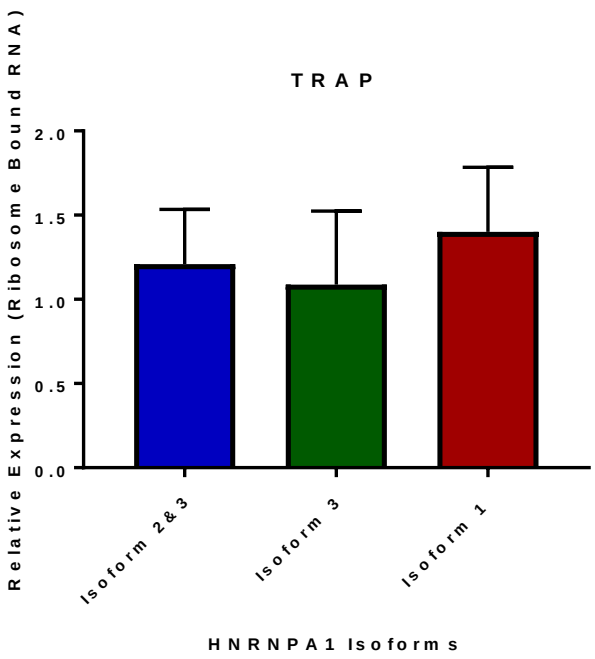

Figure 3.9 RT-qPCR result of HNRNPA1 isoforms, all RT-qPCRs were performed 35 cycles. Immunoprecipitation was performed twice. TRAP RNA normalized to untransfected HEK293 RNA, and then results were combined. N=3, every RT-qPCR contains three technical replicates. One way ANOVA was applied for statistical analysis, p=0.6268, non-significant.

We did not observe significant differences between HNRNPA1 Isoform 1, Isoform 2, and Isoform 3. In other words, all three isoforms are associated with polysomes and hence are translated. Table 3.2 shows the coding potential (probability) of HNRNPA1 Isoform1, Isoform2, Isoform3, XIST, and MALAT (CPAT, Coding Potential Assessment Tool).

Table 3.2 Coding Potential of HNRNPA1 Isoforms and lncRNAs

GENE	Ensembl ID	Coding Probability/Potential	Coding Label
HNRNPA1 Isoform 1	ENST00000547566.5	0.99902	yes
HNRNPA1 Isoform 2	ENST00000330752.12	0.9984	yes
HNRNPA1 Isoform 3	ENST00000546500.5	0.99903	yes
MALAT 1	ENST00000619449.2	0.01419	no
XIST	ENSG00000229807	0.0268	no

Overall, the TRAP method optimization has proved successful in terms of specific pull-down of ribosome-associated RNAs. We showed XIST and MALAT1 lncRNAs to be not-associated with the polysomes. However, three isoforms of a coding gene were all associated with the ribosome. This method is suitable to screen individual RNA molecules as well as high throughput analysis of translated RNAs.

CHAPTER 4

CONCLUSION

Alternative transcription start site, alternative splicing, and alternative polyadenylation generates isoforms from the same genes. These alternative transcripts can have different coding potential and ribosome occupancy. TRAP provides a detecting translation profile of a gene by targeting specific isoforms. In this study, we optimized Translating Ribosomal Affinity Purification (TRAP) in the HEK293 cell line. We started our optimization with the cloning of eGFP tagged RPL10A. We confirmed our cloning with sequencing and transient and stable transfection. After showing the expression of eGFP-RPL10A, we sorted HEK293 and MCF-7 cell lines for the separation of low and high eGFP-RPL10A expressing cells. First of all, we examined that eGFP-RPL10A fusion protein can be immunoprecipitated with magnetic bead conjugated Llama Anti-GFP VHH Single Domain Monoclonal Antibody (Magnetic Beads) (ABCAM, ab-193983). Next, we managed to immunoprecipitate polysomes with the same magnetic bead. We were successful in procuring RNA samples from TRAP. We added long non-coding RNA (lncRNA) controls for checking only, or mostly ribosome-associated mRNAs were immunoprecipitated. Consequently, we showed the specificity of the TRAP assay.

Overall, Isoform targeting may have impact in therapeutic approaches for inherited diseases and cancer. For example, BCL-X, MDM2, BRCA1, CD44, SYK, ESR1, ESR2, and TP53 genes express multiple mRNA isoforms associated with cancer subtypes (W. Zhao, Hoadley, Parker, & Perou, 2016). Targeting specific isoforms and revealing function and translation status can guide other molecular studies in light of this information. In this study, we showed the ribosome association of HNRNPA1 gene isoforms. Isoform 1, Isoform 2, and Isoform 3 of the HNRNPA1 gene associates with ribosomes and are translated. One of the most striking results of the TRAP experiment

was Isoform 1 which is erronously identified as a non-coding RNA, to be associated with ribosomes

REFERENCES

Ainsley, J. A., Drane, L., Jacobs, J., Kittelberger, K. A., & Reijmers, L. G. (2014). Functionally diverse dendritic mRNAs rapidly associate with ribosomes following a novel experience. *Nature Communications*, *5*, 1–11. https://doi.org/10.1038/ncomms5510

Akman, H. B., & Erson-bensan, A. E. (2014). *Alternative Polyadenylation and Its Impact on Cellular Processes*.

Alonso, J. M., & Stepanova, A. N. (2015). Plant Functional genomics: Methods and protocols: Second Edition. *Plant Functional Genomics: Methods and Protocols: Second Edition*, *1284*, 1–526. https://doi.org/10.1007/978-1-4939-2444-8

Bertin, B., Renaud, Y., Aradhya, R., Jagla, K., & Junion, G. (2015). TRAP-rc, Translating Ribosome Affinity Purification from Rare Cell Populations of Drosophila Embryos. *Journal of Visualized Experiments*, (103), 1–6. https://doi.org/10.3791/52985

Bertrand, E., Chartrand, P., Schaefer, M., Shenoy, S. M., Singer, R. H., & Long, R. M. (1998). *Localization of ASH1 mRNA Particles in Living Yeast*. *2*, 437–445.

Brar, G. A., & Weissman, J. S. (2015). Ribosome profiling reveals the what, when, where and how of protein synthesis. *Nature Reviews Molecular Cell Biology*, *16*(11), 651–664. https://doi.org/10.1038/nrm4069

Chao, J. A., Patskovsky, Y., Almo, S. C., & Singer, R. H. (2008). *Structural basis for the coevolution of a viral RNA – protein complex*. *15*(1), 2007–2009. https://doi.org/10.1038/nsmb1327

Chekulaeva, M., & Landthaler, M. (2016). Minireview Eyes on Translation Minireview. *Molecular Cell*, *63*(6), 918–925. https://doi.org/10.1016/j.molcel.2016.08.031

Chen, W., Jia, Q., Song, Y., Fu, H., Wei, G., & Ni, T. (2017). Alternative Polyadenylation : Methods , Findings , and Impacts. *Genomics, Proteomics & Bioinformatics*, *15*(5), 287–300. https://doi.org/10.1016/j.gpb.2017.06.001

Chen, X., & Dickman, D. (2017). Development of a tissue-specific ribosome profiling approach in Drosophila enables genome-wide evaluation of translational adaptations. In *PLoS Genetics* (Vol. 13). https://doi.org/10.1371/journal.pgen.1007117

Darzacq, X., Yao, J., Larson, D. R., Causse, Z., Bosanac, L., Turris, V. De, … Singer,

R. H. (2009). *Imaging Transcription in Living Cells*. https://doi.org/10.1146/annurev.biophys.050708.133728

David, A., Dolan, B. P., Hickman, H. D., Knowlton, J. J., Clavarino, G., Pierre, P., … Yewdell, J. W. (2012). Nuclear translation visualized by ribosome-bound nascent chain puromycylation. *The Journal of Cell Biology*, *197*(1), 45–57. https://doi.org/10.1083/jcb.201112145

Dieck, S., Kochen, L., Hanus, C., Heumüller, M., Bartnik, I., Nassim-assir, B., … Schuman, E. M. (2015). *Direct visualization of newly synthesized target proteins in situ*. *12*(5), 1–7. https://doi.org/10.1038/nmeth.3319

Dieterich, D. C., Hodas, J. J. L., Gouzer, G., Shadrin, I. Y., Ngo, J. T., Triller, A., … Schuman, E. M. (2010). t e c h n ic a l r e p o r t s In situ visualization and dynamics of newly synthesized proteins in rat hippocampal neurons. *Nature Publishing Group*, *13*(7), 897–905. https://doi.org/10.1038/nn.2580

Dougherty, J. D. (2017). The Expanding Toolkit of Translating Ribosome Affinity Purification. *The Journal of Neuroscience*, *37*(50), 12079–12087. https://doi.org/10.1523/jneurosci.1929-17.2017

Doyle, J. P., Dougherty, J. D., Heiman, M., Schmidt, E. F., Stevens, T. R., Ma, G., … Heintz, N. (2008). Application of a Translational Profiling Approach for the Comparative Analysis of CNS Cell Types. *Cell*, *135*(4), 749–762. https://doi.org/10.1016/j.cell.2008.10.029

Drane, L., Ainsley, J. A., Mayford, M. R., & Reijmers, L. G. (2014). A transgenic mouse line for collecting ribosome-bound mRNA using the tetracycline transactivator system. *Frontiers in Molecular Neuroscience*, *7*(October), 1–10. https://doi.org/10.3389/fnmol.2014.00082

Erson-bensan, A. E., & Can, T. (2016). *Alternative Polyadenylation : Another Foe in Cancer*. *2*(19), 507–517. https://doi.org/10.1158/1541-7786.MCR-15-0489

Fang, Y., Gupta, V., Karra, R., Holdway, J. E., Kikuchi, K., & Poss, K. D. (2013). Translational profiling of cardiomyocytes identifies an early Jak1/Stat3 injury response required for zebrafish heart regeneration. *Proceedings of the National Academy of Sciences*, *110*(33), 13416–13421. https://doi.org/10.1073/pnas.1309810110

Fernández-pevida, A., Kressler, D., & Cruz, J. De. (2014). *Processing of preribosomal RNA in Saccharomyces cerevisiae*. *1*. https://doi.org/10.1002/wrna.1267

Fernie, A. R., & Schippers, J. H. M. (2012). *Translatome and metabolome effects triggered by gibberellins during rosette growth in Arabidopsis*. *63*(7), 2769–2786. https://doi.org/10.1093/jxb/err463

Floor, S. N., Doudna, J. A., States, U., & Initiative, I. G. (2016). *Tunable protein synthesis by transcript isoforms in human cells*. *4*, 1–25. https://doi.org/10.7554/eLife.10921

Fromont-Racine, M., Senger, B., Saveanu, C., & Fasiolo, F. (2003). Ribosome assembly in eukaryotes. *Gene*, *313*(1–2), 17–42. https://doi.org/10.1016/S0378-1119(03)00629-2

Gobet, C., & Naef, F. (2017). Ribosome profiling and dynamic regulation of translation in mammals. *Current Opinion in Genetics and Development*, *43*, 120–127. https://doi.org/10.1016/j.gde.2017.03.005

Gong, X., Zhang, L., Kim, G. B., & Matthew, R. (2018). In utero electroporation-based translating ribosome affinity purification identifies age-dependent mRNA expression in cortical pyramidal neurons. *Neuroscience Research*. https://doi.org/10.1016/j.neures.2018.05.006

Halbeisen, R. E. (2009). *Stress-Dependent Coordination of Transcriptome and Translatome in Yeast*. *7*(5). https://doi.org/10.1371/journal.pbio.1000105

Halbeisen, R. E., Scherrer, T., & Gerber, A. P. (2009). Affinity purification of ribosomes to access the translatome. *Methods*, *48*(3), 306–310. https://doi.org/10.1016/j.ymeth.2009.04.003

Halstead, J. M., Wilbertz, J. H., Wippich, F., & Ephrussi, A. (2015). *An RNA biosensor for imaging the first round of translation from single cells to living animals*. *347*(6228).

Hattori, D., Millard, S. S., Wojtowicz, W. M., & Zipursky, S. L. (2008). *Dscam-Mediated Cell Recognition Regulates Neural Circuit Formation*. https://doi.org/10.1146/annurev.cellbio.24.110707.175250

Heiman, M., Kulicke, R., Fenster, R. J., Greengard, P., & Heintz, N. (2014). Cell type-specific mRNA purification by translating ribosome affinity purification (TRAP). *Nature Protocols*, *9*(6), 1282–1291. https://doi.org/10.1038/nprot.2014.085

Heiman, M., Schaefer, A., Gong, S., Peterson, J. D., Day, M., Ramsey, K. E., … Heintz, N. (2008). A translational profiling approach for the molecular characterization of CNS cell types. *Cell*, *135*(4), 738–748. https://doi.org/10.1016/j.cell.2008.10.028

Housley, M. P., Reischauer, S., Dieu, M., Raes, M., Stainier, D. Y. R., & Vanhollebeke, B. (2014). Translational profiling through biotinylation of tagged ribosomes in zebrafish. *Development*, *141*(20), 3988–3993. https://doi.org/10.1242/dev.111849

Inada, T., Winstall, E., Tarun, S. Z., Yates, J. R., Schieltz, D., & Sachs, A. B. (2017).

One-step affinity purification of the yeast ribosome and its associated proteins and mRNAs. (2002), 948–958.

Ingolia, N. T., Brar, G. A., Rouskin, S., Mcgeachy, A. M., & Weissman, J. S. (2012). *The ribosome profiling strategy for monitoring translation in vivo by deep sequencing of ribosome-protected mRNA fragments*. https://doi.org/10.1038/nprot.2012.086

Jan, C. H., Jan, C. H., Williams, C. C., & Weissman, J. S. (2014). *Principles of ER cotranslational translocation revealed by proximity- specific ribosome profiling*. https://doi.org/10.1126/science.1257521

Jiao, Y., & Meyerowitz, E. M. (2010). Cell-type specific analysis of translating RNAs in developing flowers reveals new levels of control. *Molecular Systems Biology*, *6*(419), 1–14. https://doi.org/10.1038/msb.2010.76

Juntawong, P., & Bailey-serres, J. (2012). *Dynamic light regulation of translation status in Arabidopsis thaliana*. *3*(April), 1–16. https://doi.org/10.3389/fpls.2012.00066

Kahles, A., Lehmann, K. Van, Toussaint, N. C., Hüser, M., Stark, S. G., Sachsenberg, T., … Rätsch, G. (2018). Comprehensive Analysis of Alternative Splicing Across Tumors from 8,705 Patients. *Cancer Cell*, *34*(2), 211-224.e6. https://doi.org/10.1016/j.ccell.2018.07.001

Lafontaine, D. L. J. (2015). *RE V IE W Noncoding RNAs in eukaryotic ribosome biogenesis and function*. *22*(1), 11–19. https://doi.org/10.1038/nsmb.2939

Licatalosi, D. D., & Darnell, R. B. (2010). RNA processing and its regulation : global insights into biological networks. *Nature Reviews Genetics*, *11*, 75–87. https://doi.org/10.1038/nrg2673

Liu, J., Krautzberger, a M., Sui, S. H., Hofmann, O. M., Chen, Y., Baetscher, M., … Mcmahon, A. P. (2014). *Technical advance Cell-speci fi c translational pro fi ling in acute kidney injury*. *124*(3). https://doi.org/10.1172/JCI72126DS1

Mayr, C., & Bartel, D. P. (2009). Widespread Shortening of 3 0 UTRs by Alternative Cleavage and Polyadenylation Activates Oncogenes in Cancer Cells. *Cell*, *138*(4), 673–684. https://doi.org/10.1016/j.cell.2009.06.016

Merkin, J. (2012). *Evolutionary Dynamics of Gene*. *1593*. https://doi.org/10.1126/science.1228186

Moeller, J. R., Moscou, M. J., Bancroft, T., Skadsen, R. W., Wise, R. P., & Whitham, S. A. (2012). *Molecular BioSystems Differential accumulation of host mRNAs on polyribosomes during obligate pathogen-plant interactions w*. 2153–2165. https://doi.org/10.1039/c2mb25014d

Morin, X., Daneman, R., Zavortink, M., & Chia, W. (2001). A protein trap strategy to detect GFP-tagged proteins expressed from their endogenous loci in Drosophila. *Proceedings of the National Academy of Sciences*, *98*(26), 15050–15055. https://doi.org/10.1073/pnas.261408198

Morisaki, T., Lyon, K., Deluca, K. F., Deluca, J. G., English, B. P., Lavis, L. D., … Stasevich, T. J. (2016). *Real-time quantification of single RNA translation dynamics in living cells*. *0899*, 1–10.

Mustroph, A., Zanetti, M. E., Jang, C. J. H., Holtan, H. E., Repetti, P. P., Galbraith, D. W., … Bailey-serres, J. (2009). *Profiling translatomes of discrete cell populations resolves altered cellular priorities during hypoxia in Arabidopsis*. *106*(44).

Palasin, K., Uechi, T., Yoshihama, M., Srisowanna, N., Choijookhuu, N., Hishikawa, Y., … Chotigeat, W. (2019). *Abnormal development of zebrafish after knockout and knockdown of ribosomal protein L10a.pdf*. https://doi.org/10.1038/s41598-019-54544-w

Sanz, E., Yang, L., Su, T., Morris, D. R., Mcknight, G. S., & Amieux, P. S. (2009). *Cell-type-specific isolation of ribosome-associated mRNA from complex tissues*. *106*(33), 13939–13944.

Schmidt, E. F., Warner-schmidt, J. L., Otopalik, B. G., Pickett, S. B., & Greengard, P. (2012). Identification of the Cortical Neurons that Mediate Antidepressant Responses. *Cell*, *149*(5), 1152–1163. https://doi.org/10.1016/j.cell.2012.03.038

Schmidt, E. K., Clavarino, G., Ceppi, M., & Pierre, P. (2009). *SUnSET , a nonradioactive method to monitor protein synthesis*. *6*(4), 275–277. https://doi.org/10.1038/NMETH.1314

Shi, Z., Fujii, K., Kovary, K. M., Genuth, N. R., Ro¨ st, H. L., Teruel, M. N., & Barna, M. (2017). *Heterogeneous Ribosomes Preferentially Translate.pdf* (pp. 71–83). pp. 71–83. https://doi.org/https://doi.org/10.1016/j.molcel.2017.05.021

Tanenbaum, M. E., Gilbert, L. A., Qi, L. S., Weissman, J. S., & Vale, R. D. (2014). Resource A Protein-Tagging System for Signal Amplification in Gene Expression and Fluorescence Imaging. *Cell*, *159*(3), 635–646. https://doi.org/10.1016/j.cell.2014.09.039

Tian, B., Hu, J., Zhang, H., & Lutz, C. S. (2005). *A large-scale analysis of mRNA polyadenylation of human and mouse genes*. *33*(1), 201–212. https://doi.org/10.1093/nar/gki158

Tollervey, D., & Kos, M. (2010). Article Yeast Pre-rRNA Processing and Modification Occur Cotranscriptionally. *Molecular Cell*, *37*(6), 809–820. https://doi.org/10.1016/j.molcel.2010.02.024

Tschochner, H., & Hurt, E. (2003). Pre-ribosomes on the road from the nucleolus to the cytoplasm. *Trends in Cell Biology*, *13*(5), 255–263. https://doi.org/10.1016/S0962-8924(03)00054-0

Ule, J., & Darnell, R. B. (2006). *RNA binding proteins and the regulation of neuronal synaptic plasticity*. 102–110. https://doi.org/10.1016/j.conb.2006.01.003

Van Riggelen, J., Yetil, A., & Felsher, D. W. (2010). MYC as a regulator of ribosome biogenesis and protein synthesis. *Nature Reviews Cancer*, *10*(4), 301–309. https://doi.org/10.1038/nrc2819

Visanji, N. P., & Sarvestani, I. K. (2015). *Deep brain stimulation of the subthalamic nucleus preferentially alters the translational profile of striatopallidal neurons in an animal model of Parkinson ' s disease*. *9*(June), 1–11. https://doi.org/10.3389/fncel.2015.00221

Wang, E., & Aifantis, I. (2020). RNA Splicing and Cancer. *Trends in Cancer*, 1–14. https://doi.org/10.1016/j.trecan.2020.04.011

Watson, F. L., Mills, E. A., Wang, X., Guo, C., & Chen, D. F. (2012). *Cell Type – Specific Translational Profiling in the Xenopus laevis Retina*. (October), 1960–1972. https://doi.org/10.1002/dvdy.23880

Wellmer, F. (2016). Flower Development. *Encyclopedia of Applied Plant Sciences*, *2*, 269–274. https://doi.org/10.1016/B978-0-12-394807-6.00042-3

Wonglapsuwan, M., Chotigeat, W., Timmons, A., & McCall, K. (2011). *RpL10A Regulates Oogenesis Progression in the Banana Prawn Fenneropenaeus Merguiensis and Drosophila Melanogaster.pdf* (pp. 356–363). pp. 356–363. https://doi.org/10.1016/j.ygcen.2011.06.012

Yan, X., Hoek, T. A., Vale, R. D., Tanenbaum, M. E., Yan, X., Hoek, T. A., … Tanenbaum, M. E. (2016). *Dynamics of Translation of Single mRNA Molecules In Vivo Resource Dynamics of Translation of Single mRNA Molecules In Vivo*. 976–989. https://doi.org/10.1016/j.cell.2016.04.034

Zhao, D., Hamilton, J. P., Hardigan, M., Yin, D., He, T., Vaillancourt, B., … Jiang, N. (2017). Analysis of Ribosome-Associated mRNAs in Rice Reveals the Importance of Transcript Size and GC Content in Translation. *G3: Genes|Genomes|Genetics*, *7*(1), 203–219. https://doi.org/10.1534/g3.116.036020

Zhao, J., Qin, B., Nikolay, R., Spahn, C. M. T., & Zhang, G. (2019). *Translatomics : The Global View of Translation*. https://doi.org/10.3390/ijms20010212

APPENDICES

A. BUFFERS AND SOLUTIONS

6X SDS Loading Buffer

0,35M Tris-HCl pH:6,8

10,28% (w/v) SDS

36% (v/v) glycerol

5% β-mercaptoethanol

0,0012% (w/v) Bromophenol Blue

1X PBS

137mM NaCl

2,7mM KCl

10mM Na2HPO4.2H2O

2mM KH2PO4

Lysis Buffer

10 mM Tris-HCl ph:7.5

150 mM NaCl

100 mM MgCl2

0.5% NP-40

1X Protease Inhibitor

1X Phos-Stop

100ug/mL CHX

Wash Buffer

10 mM Tris-HCl ph:7.5

150 mM NaCl

100 mM MgCl

1X Protease Inhibitor

1X Phos-Stop

100ug/mL CHX

10% Separating Gel

3.33 ml Acrylamide-Bisacrylamide

2.5 ml 1.5 M Tris-HCl pH:8.8

100 µl SDS (10%)

100 µl APS (10%)

4ul TEMED

3.96 ml dH_2O

5% Stacking Gel

1.36 ml Acrylamide-Bisacrylamide

1 ml 1M Tris-HCl pH:6.8

80 µl SDS (10%)

80 µl APS (10%)

8ul TEMED

5.44 ml dH2O

TBS-T

20 mM Tris

137 mM NaCl

0.1% Tween 20

pH:7.6

10X Running Buffer

25 mM Tris base

190 mM Glycine

0.1% SDS

Dilute 1X with dH2O

B. VECTOR CONSTRUCT

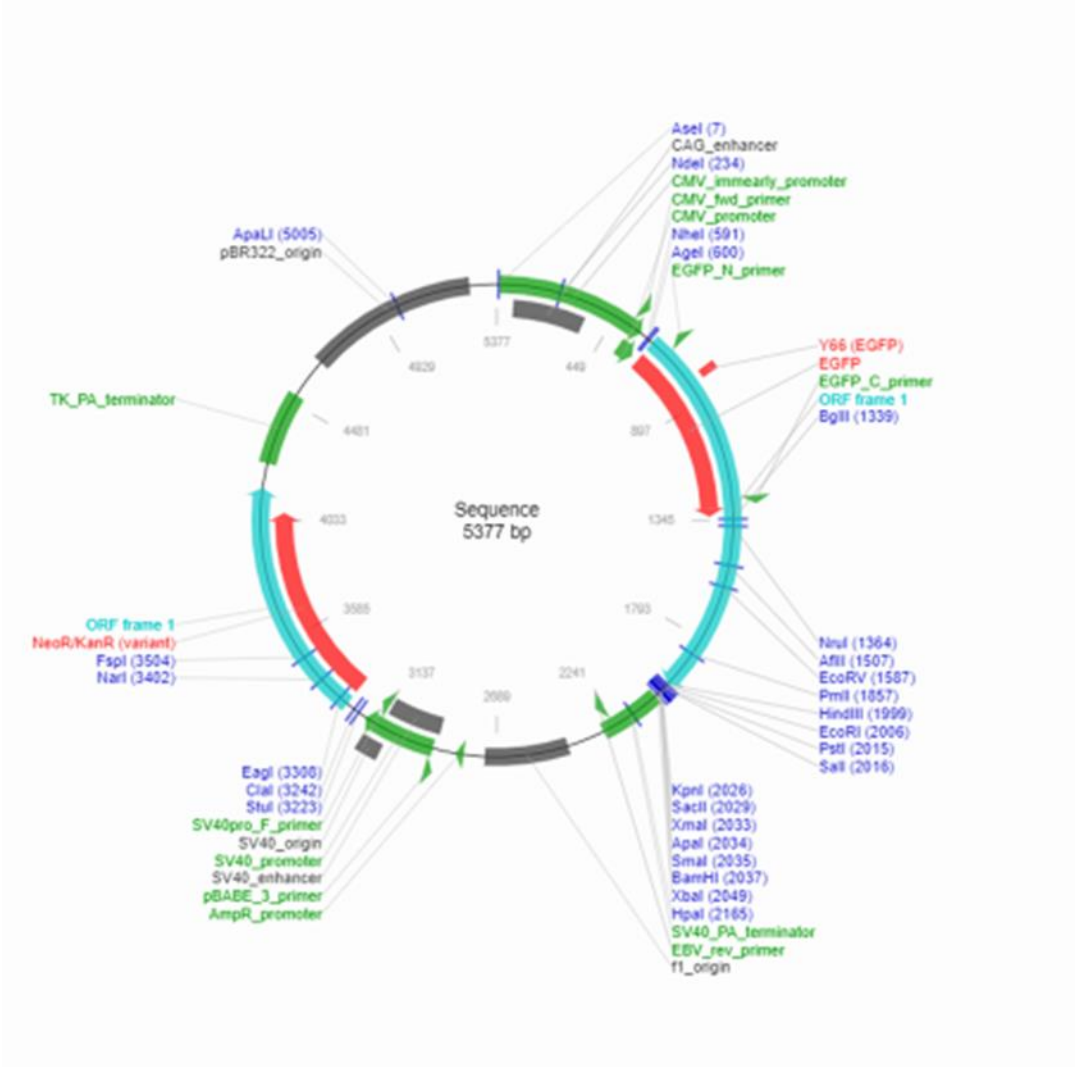

Figure 4.1 Vector construct after cloning of RPL10A to pEGFP-C1 vector

C. CLONING SEQUENCE RESULTS

Score	Expect	Identities	Gaps	Strand
1642 bits(889)	0.0	889/889(100%)	0/889(0%)	Plus/Plus

```
Query  1    AGCAAAGACCCCAACGAGAAGCGCGATCACATGGTCCTGCTGGAGTTCGTGACCGCCGCC  60
Sbjct  1    AGCAAAGACCCCAACGAGAAGCGCGATCACATGGTCCTGCTGGAGTTCGTGACCGCCGCC  60

Query  61   GGGATCACTCTCGGCATGGACGAGCTGTACAAGTCCGGACTCAGATCTATGAGCAGCAAA  120
Sbjct  61   GGGATCACTCTCGGCATGGACGAGCTGTACAAGTCCGGACTCAGATCTATGAGCAGCAAA  120

Query  121  GTCTCTCGCGACACCCTGTACGAGGCGGTGCGGGAAGTCCTGCACGGGAACCAGCGCAAG  180
Sbjct  121  GTCTCTCGCGACACCCTGTACGAGGCGGTGCGGGAAGTCCTGCACGGGAACCAGCGCAAG  180

Query  181  CGCCGCAAGTTCCTGGAGACGGTGGAGTTGCAGATCAGCTTGAAGAACTATGATCCCCAG  240
Sbjct  181  CGCCGCAAGTTCCTGGAGACGGTGGAGTTGCAGATCAGCTTGAAGAACTATGATCCCCAG  240

Query  241  AAGGACAAGCGCTTCTCGGGCACCGTCAGGCTTAAGTCCACTCCCCGCCCTAAGTTCTCT  300
Sbjct  241  AAGGACAAGCGCTTCTCGGGCACCGTCAGGCTTAAGTCCACTCCCCGCCCTAAGTTCTCT  300

Query  301  GTGTGTGTCCTGGGGGACCAGCAGCACTGTGACGAGGCTAAGGCCGTGGATATCCCCCAC  360
Sbjct  301  GTGTGTGTCCTGGGGGACCAGCAGCACTGTGACGAGGCTAAGGCCGTGGATATCCCCCAC  360

Query  361  ATGGACATCGAGGCGCTGAAAAAACTCAACAAGAATAAAAAACTGGTCAAGAAGCTGGCC  420
Sbjct  361  ATGGACATCGAGGCGCTGAAAAAACTCAACAAGAATAAAAAACTGGTCAAGAAGCTGGCC  420

Query  421  AAGAAGTATGATGCGTTTTTGGCCTCAGAGTCTCTGATCAAGCAGATTCCACGAATCCTC  480
Sbjct  421  AAGAAGTATGATGCGTTTTTGGCCTCAGAGTCTCTGATCAAGCAGATTCCACGAATCCTC  480

Query  481  GGCCCAGGTTTAAATAAGGCAGGAAAGTTCCCTTCCCTGCTCACACACAACGAAAACATG  540
Sbjct  481  GGCCCAGGTTTAAATAAGGCAGGAAAGTTCCCTTCCCTGCTCACACACAACGAAAACATG  540

Query  541  GTGGCCAAAGTGGATGAGGTGAAGTCCACAATCAAGTTCCAAATGAAGAAGGTGTTATGT  600
Sbjct  541  GTGGCCAAAGTGGATGAGGTGAAGTCCACAATCAAGTTCCAAATGAAGAAGGTGTTATGT  600

Query  601  CTGGCTGTAGCTGTTGGTCACGTGAAGATGACAGACGATGAGCTTGTGTATAACATTCAC  660
Sbjct  601  CTGGCTGTAGCTGTTGGTCACGTGAAGATGACAGACGATGAGCTTGTGTATAACATTCAC  660

Query  661  CTGGCTGTCAACTTCTTGGTGTCATTGCTCAAGAAAAACTGGCAGAATGTCCGGGCCTTA  720
Sbjct  661  CTGGCTGTCAACTTCTTGGTGTCATTGCTCAAGAAAAACTGGCAGAATGTCCGGGCCTTA  720

Query  721  TATATCAAGAGCACCATGGGCAAGCCCCAGCGCCTATATTAAAAGCTTCGAATTCTGCAG  780
Sbjct  721  TATATCAAGAGCACCATGGGCAAGCCCCAGCGCCTATATTAAAAGCTTCGAATTCTGCAG  780

Query  781  TCGACGGTACCGCGGGCCCGGGATCCACCGGATCTAGATAACTGATCATAATCAGCCATA  840
Sbjct  781  TCGACGGTACCGCGGGCCCGGGATCCACCGGATCTAGATAACTGATCATAATCAGCCATA  840

Query  841  CCACATTTGTAGAGGTTTTACTTGCTTTAAAAAACCTCCCACACCTCCC  889
Sbjct  841  CCACATTTGTAGAGGTTTTACTTGCTTTAAAAAACCTCCCACACCTCCC  889
```

Figure 4.2 Sequencing Results of pEGFP-C1_RPL10A cloning.

D. STATISTICS OF GFP CELL SORTING

STATISTICS

Population	Events	% Parent	% Total	FSC-A Median	FSC-A %rCV	SSC-A Median	SSC-A %rCV
All Events	2,000		100.00 %	67358.86	25.62 %	36648.77	37.85 %
Scatter	1,967	98.35 %	98.35 %	67198.20	25.23 %	36273.55	36.91 %
SSC Singlets	1,695	86.17 %	84.75 %	64907.35	21.09 %	33960.30	31.39 %
FSC Singlets	1,695	100.00 %	84.75 %	64907.35	21.09 %	33960.30	31.39 %
P1-1	0	0.00 %	0.00 %				
P1-2	1,349	79.59 %	67.45 %	65226.38	20.92 %	34376.55	31.59 %
P1-3	0	0.00 %	0.00 %				
P1-4	346	20.41 %	17.30 %	63896.62	22.70 %	32201.67	29.28 %
P2	742	43.78 %	37.10 %	65585.93	20.21 %	35842.01	32.61 %
P3	486	28.67 %	24.30 %	63587.86	21.55 %	32893.19	29.88 %

Figure 4.3 Statistical values of eGFP-L10A expressing HEK293 cell sorting

E. RT-qPCR ANALYSIS RESULTS

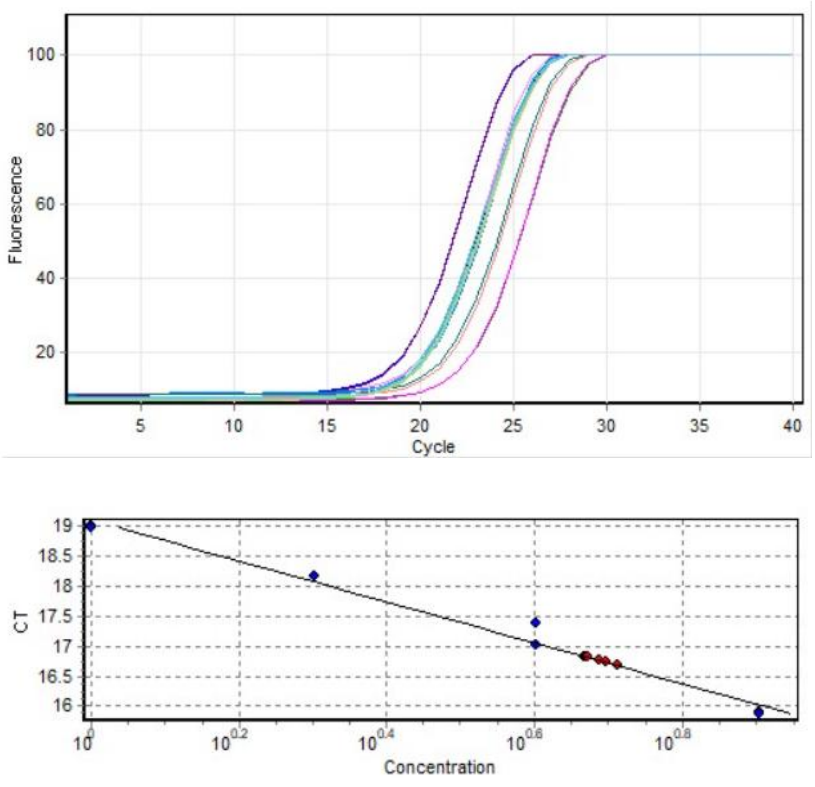

Figure 4.4 Raw data and standard curve of RPLP0 RT-Qpcr

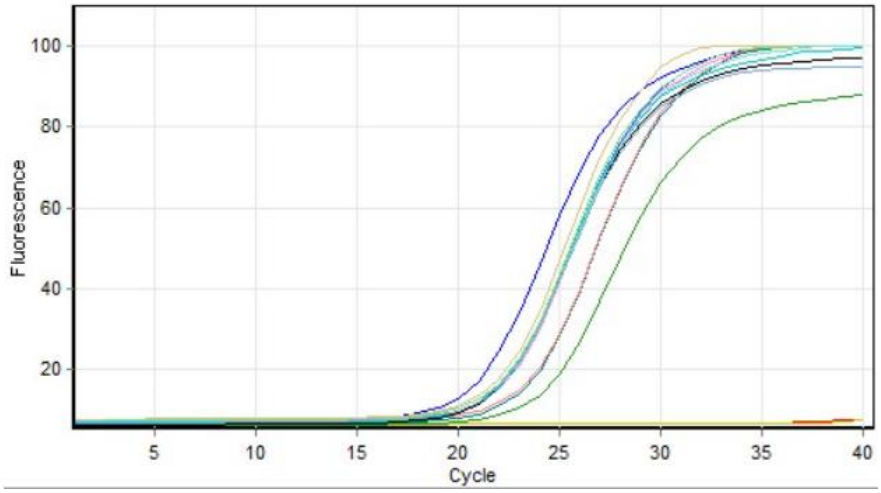

Standard Curve

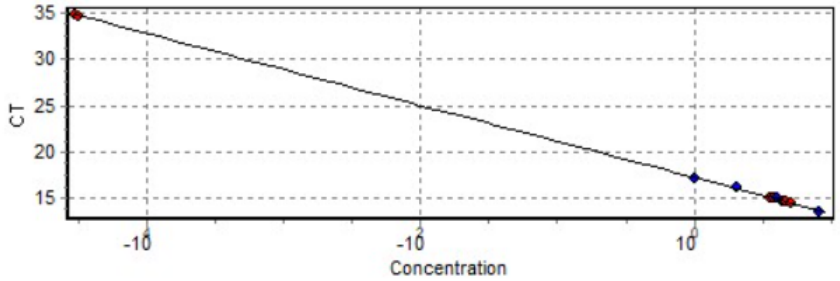

Figure 4.5 Raw data and standard curve of Isoform 2&3 RT-qPCR

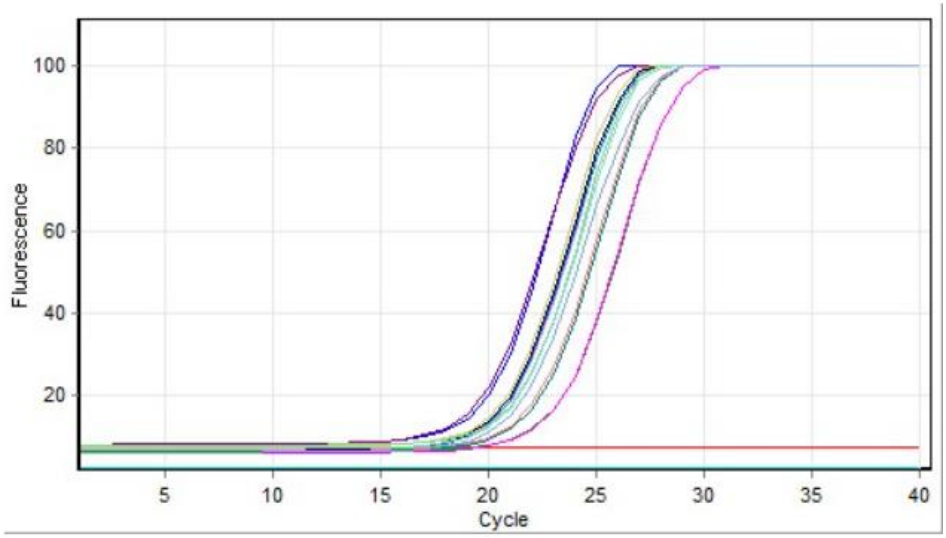

Standard Curve

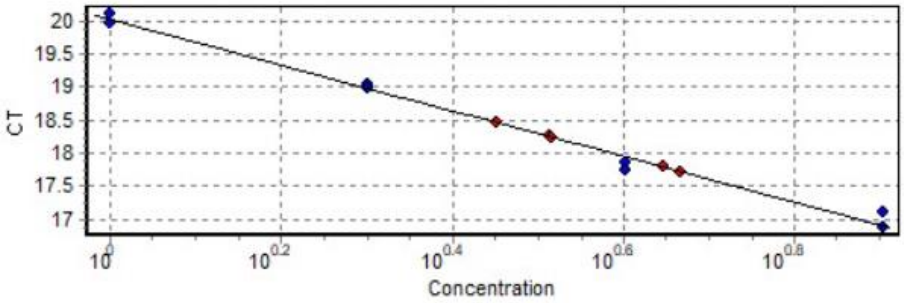

Figure 4.6 Raw data and standard curve of Isoform 3 RT-qPCR

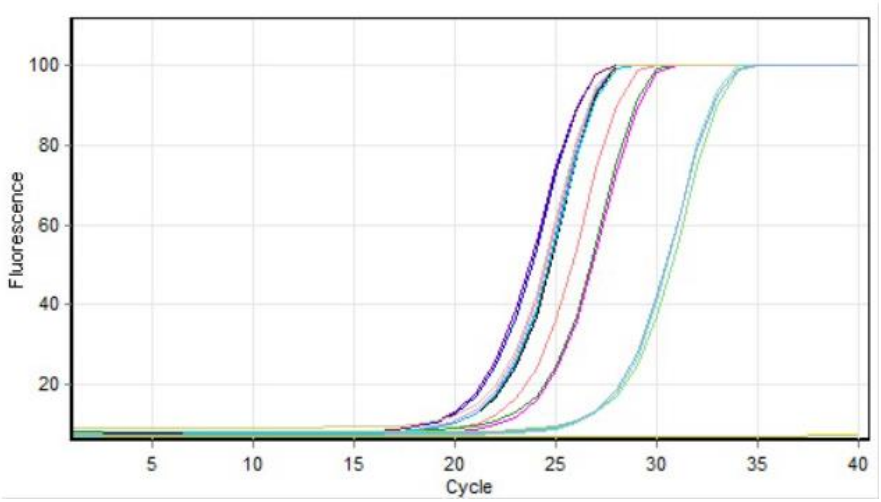

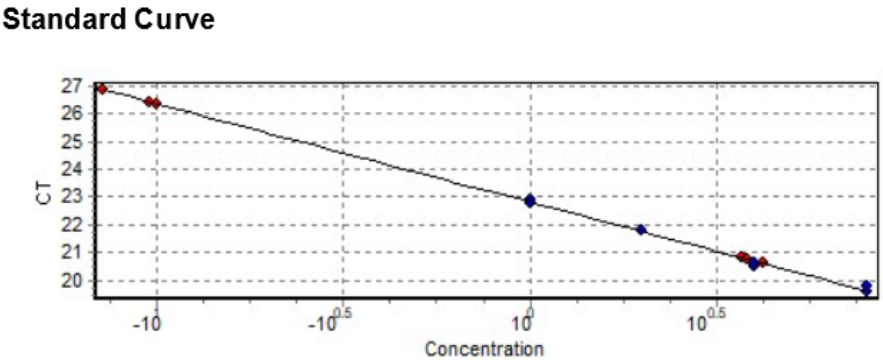

Figure 4.7 Raw data and standard curve of XIST RT-qPCR